energies

Article

Evaluating Traffic-Calming-Based Urban Road Design Solutions Featuring Cooperative Driving Technologies in Energy Efficiency Transition for Smart Cities

Maria Luisa Tumminello [1,*], Elżbieta Macioszek [2,*], Anna Granà [1,3] and Tullio Giuffrè [4]

[1] Department of Engineering, University of Palermo, Viale delle Scienze ed 8, 90128 Palermo, Italy; anna.grana@unipa.it
[2] Department of Transport Systems, Traffic Engineering and Logistics, Faculty of Transport and Aviation Engineering, Silesian University of Technology, Krasińskiego 8 Street, 40-019 Katowice, Poland
[3] Sustainable Mobility Center (Centro Nazionale per la Mobilità Sostenibile—CNMS), Via Giovanni Durando, 39, 20158 Milano, Italy
[4] Faculty of Engineering and Architecture, University of Enna Kore, Viale della Cooperazione, 94100 Enna, Italy; tullio.giuffre@unikore.it
* Correspondence: marialuisa.tumminello01@unipa.it (M.L.T.); elzbieta.macioszek@polsl.pl (E.M.)

Abstract: Traffic-calming measures (TCMs) are non-invasive devices designed to improve road mobility and urban areas on a human scale. Despite their potential, they have been in use for a long time and now have to deal with the latest technological innovations in the automotive field, such as cooperative driving technologies (CDTs), to improve energy efficiency in cities. The goal of this study is to explore the safety and operational performances of TCMs featuring CDTs in urban areas. An urban-scale road network close to a seaside area in the City of Mazara del Vallo, Italy, was properly redesigned and simulated in AIMSUN to assess several design solutions, where connected and automated vehicles (CAVs) have been employed as a more energy-efficient public transportation system. Preliminarily, the fine-tuning process of model parameters included CAVs and human-operated vehicles (HOVs) flowing through the network up to saturation conditions. The safety of the planned solutions was tested by using surrogate measures. The micro-simulation approach allowed us to know in advance and compare the operational and safety performances of environmentally friendly solutions involving TCMs and CDTs. These results can also support urban road decision makers in pivoting urban-traffic-calming-based design solutions featuring cooperative driving technologies toward energy efficiency transitions for smart cities.

Keywords: traffic-calming measures; connected and autonomous vehicles; roundabouts; limited traffic zone; Aimsun Next; urban metabolism; energy efficiency; surrogate measures of safety; smart cities

check for updates

Citation: Tumminello, M.L.; Macioszek, E.; Granà, A.; Giuffrè, T. Evaluating Traffic-Calming-Based Urban Road Design Solutions Featuring Cooperative Driving Technologies in Energy Efficiency Transition for Smart Cities. *Energies* **2023**, *16*, 7325. https://doi.org/10.3390/en16217325

Academic Editor: Andrea Mariscotti

Received: 6 September 2023
Revised: 19 October 2023
Accepted: 21 October 2023
Published: 29 October 2023

1. Introduction

Following the demands of a new urban metabolism and mobility in increasingly energy-efficient and smart cities, today, several researchers and practitioners in the road engineering field have been called to design safe and functional solutions, combining the needs of citizens and road users, as well as to manage their relationship with the built environment. In a bid to deliver better mobility conditions to road users, traffic-calming measures (TCMs) are considered to be a winning strategy to increase the well-being of citizens in urban spaces. Indeed, TCMs are useful and non-invasive devices aimed at lowering energy consumption and other adverse effects of motorized traffic, reducing the need for idling at traffic lights or stop signs, which can waste fuel, and forcing drivers to adopt a more responsible and careful driving behavior toward non-motorized road users with whom they share urban road spaces [1]. TCMs include traffic management and design solutions for regulating the accessibility in a given urban area as well as a wide variety of road devices for the reduction in and control of vehicular speeds so that slower driving speeds may result in better fuel efficiency. In field applications, these measures consist of the adoption of vertical speed control devices, such as speed humps, speed lumps, and speed tables; the creation of textured pavements; the installation of chicanes, later shifts, and narrowings; and so on [2]. TCMs also provide traffic zones or pedestrian areas that prevent or limit access to certain road spaces to certain categories of vehicles at specific time slots. From this point of view, roundabouts are considered a useful tool to moderate traffic flows [3,4]. The above-mentioned measures have the primary effect of reducing vehicle speeds and, consequently, a series of benefits linked to it, such as a decrease in the number of road crashes and their severity, the mitigation of vehicular noise and emissions, an improvement in air quality and energy efficiency, and the optimization of spaces designed for shared mobility. Efficiently designing and applying these measures, in a nutshell, means making urban road spaces more livable for people and well harmonized with the surrounding landscape. Moreover, citizen and tourist perceptions of safe, functional, and aesthetically appealing urban spaces in a technologically abreast-of-the-times city are not an aspect to be neglected since they can encourage road users to use sustainable and environmentally friendly forms of mobility.

In the last decade, we are witnessing the transition toward increasingly smart and energy-efficient cities. Although TCMs have been in use for a long time, they now have to deal with the latest technological innovations in the automotive field, such as cooperative driving technologies (CDTs). Indeed, connected and automated vehicles (CAVs) seem to be one of the most promising elements of intelligent transport systems (ITSs) in support of the development of smart and energy-efficient cities with the potential to significantly improve the mobility conditions of road users and, consequently, the general quality of life in urban cities [5]. The development of sustainable mobility in smart cities, under various aspects, cannot prescind the use of CDTs, the potential of which could be combined with TCMs to improve their expected benefits [6]. In this regard, some researchers have reached the conclusion that CAVs could increase road safety, improve operation conditions, and reduce environmental pollution and energy consumption [7,8]—all benefits that are in line with the objectives of TCMs. CAV technology should replace the driver in all aspects, starting from dynamic situations in all conditions and roads, both in simple traffic scenarios and more complex traffic situations. Indeed, traffic scenarios that are configured in urban contexts with high traffic volumes may represent hard situations for CAVs to navigate, considering the high degree of interactions with human-operated vehicles (HOVs), public transport, or other road users, like pedestrians, cyclists, or kick scooters. However, the curvilinear geometry of roundabouts can represent another trickly condition for CAVs: CAVs approaching a roundabout must apply priority rules and negotiate antagonist circulating traffic before entering; in turn, the deviations in the trajectories inflicted on CAVs via TCMs may represent difficult situations to manage. In the era of cities in transition, it would be interesting to know how CAVs run in urban road networks in which TCMs are installed and what contribution they can make to increasing or integrating their benefits.

The Aim of this Study

Starting from the above considerations, the goal of this study is to explore the operational and safety performances in an urban setting, where TCMs and CDTs are combined. In this regard, the tourist-oriented urban area in the City of Mazara del Vallo, Italy, was chosen as a case study. Hence, the road network near the seaside area was redesigned by adjusting lane width, implementing a limited traffic zone (LTZ), and adding roundabouts as TCMs.

In a microsimulation environment, Aimsun Next [9] was used to evaluate the feasibility of three road solutions (referred to as Project Solutions 1 to 3). These solutions incorporated energy-efficient CAVs as part of the public transportation system in a seaside area. The study involved simulating each Project Solution under two different traffic scenarios (Traffic Scenarios A and B) to assess their operational performance and environmental impact when employing a combination of TCMs and CDTs. Furthermore, the study evaluated the potential safety benefits of urban road design solutions with CDTs by analyzing trajectory data and using the Surrogate Safety Assessment Model (SSAM) [10].

The exploratory study on the potential benefits of TCMs featuring CDTs employed a micro-simulation approach to compare each of the three conceptualized design solutions with the current state of the examined road network. The evaluation aimed to assess the operational, safety, and energy-efficient performance of each proposed design solution, focusing on factors such as delays and the number of potential conflicts. Furthermore, the study considered the environmental impact resulting from vehicular emissions generated by mobile sources. The model parameters related to CAVs were accurately calibrated in Aimsun Next to replicate their real driving behavior. Additionally, the implementation of an LTZ had the primary effect of reducing traffic flow through the road network during specific time slots. As expected, the micro-simulation recorded improvements in both operational and safety conditions as well as a reduction in vehicular emissions during time slots that restricted the entry of certain traffic categories.

The results have demonstrated the effectiveness of a simulation-based approach in shaping urban mobility strategies and designing road-shared spaces that are not only attractive to citizens and tourists but also enhance the overall quality of daily life and well-being for urban road users. Among the three conceptualized design alternatives, Project Solution 3 (PS3) emerged as the most promising option in terms of environmental impact and operational performance. In the simulation environment, PS3 exhibited the most significant reductions in delays and polluting emissions compared to the existing conditions. The safety analysis, conducted through surrogate safety measures, also confirmed PS3's higher performance. In light of evolving urban planning and road development objectives, the micro-simulation approach can guide decision makers in adopting traffic-calming design solutions that incorporate energy-efficient CDTs. Also, the hypotheses underlying the three design solutions in this case study represent a feasibility study. Further support is required from an in-depth market investigation to understand how people may embrace CDTs and behave in CAVs.

The framework presented in Figure 1 illustrates the simulation-based approach proposed for the case study discussed in this paper.

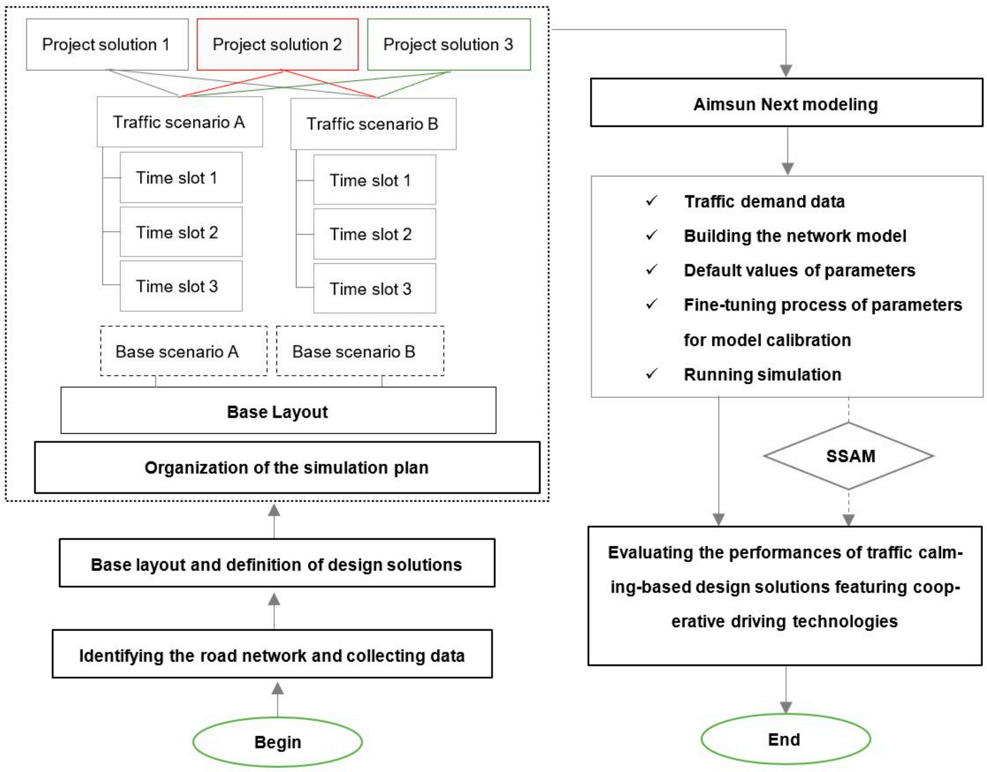

Figure 1. Methodological framework to assess performances of traffic-calming-based design solutions featuring cooperative driving technologies framework.

The organization of the paper is as follows: Section 2 presents the related research on the topic to explain how to address the knowledge gap in the current literature; Section 3 presents the materials and methods applied in the research, while Section 4 presents the results. Finally, the results are discussed in Section 5, and Section 6 concludes the paper, highlighting future research developments.

2. Related Research

The benefits of TCMs are generally associated with the prevention of road traffic injuries, increased road safety, improved environmental quality, energy savings, aesthetic enhancements, and the functional optimization of public spaces [11,12]. Several studies have explored the effects of TCMs on speed reduction [3] and their impact on road safety at both the neighborhood and urban-wide scales [13–16]. The impact of redesigning road spaces with TMCs at the neighborhood level has also highlighted their role in developing sustainable urban mobility plans [17]. While some studies have indicated that TCMs can complicate the assessment of operational and safety conditions in simulation environments, there is no doubt that these measures lay the foundation for improving the quality of life in neighborhoods [18]. A meta-analysis conducted on a citywide scale concluded that TMCs reduce the number of crashes, especially on residential streets as compared to main roads [19]. Regarding the type of device, another study investigated the effects of combining TMCs (e.g., speed bumps, speed humps, raised crosswalks), safety islands, and speed cameras on reducing the number of injuries [20]. The results revealed that the number of injuries decreased by 63% where TMCs causing vertical shifts were implemented. Moreover, the number of injuries decreased by 78% where safety islands with horizontal marking and flexible reflective posts were installed.

The effectiveness of various aspects of traffic-calming devices, whether used in combination or individually, has been explored in several research studies. In this regard, Lee et al. [21] used a micro-simulation model to assess the impact of chicanes on reducing vehicular speeds and their implications for energy and fuel consumption. In turn, Ariën et al. [22] employed a driving simulator to investigate the safety efficiency of curves and gates as access control measures on major roads, evaluating their influence on driving behavior and workload. The authors emphasized that the safety benefits of the examined TMCs were contingent on the specific context of installation, and further studies were necessary to provide generalizable results.

Di Stefano and Leonardi [23] compared the effects of speed tables, chicanes, and road narrowing on speed reduction. Their results revealed that speed tables had the most pronounced impact on reducing speeds, halving the average speed. Chicanes and speed tables also reduced average speeds by up to 50%, while road narrowing led to a 35% reduction in average speed. All three traffic-calming measures contributed to a reduction in crashes of more than 30%. Similar results were obtained by Aydin et al. [24]; they conducted a study to classify and compare the safety performance of various types of chicanes located on two- and four-lane streets using a driving simulator. The operational performance of TCMs, such as flat-topped humps, single bumps, and double bumps located on arterial roads, was examined using video cameras and speed radar guns [25]. The authors used acceleration noise to measure speed changes and found higher values attributed to flat-topped humps. Conversely, the highest delay was recorded for double-speed bumps. When analyzing various TCMs, Gonzalo-Orden et al. [13] noted that the raised crosswalk and lane narrowing exhibited the best performance in reducing vehicular speeds. However, the authors observed an improvement in speed reduction effectiveness when TCMs were combined and applied in close proximity to each other. Moreover, the relationship between the reduction in speed and the relative distance among different traffic-calming devices has been studied by several researchers. An important finding is that the speed reduction effect caused by TCMs may diminish immediately after the devices have been passed [26]. To ensure the efficiency of TCMs both at the neighborhood and urban levels, they should be grouped and applied consecutively with a certain spacing between them to prevent vehicular speeds from exceeding the imposed limits [27]. This issue has also been examined by [26], whose results indicated increased values of vehicular speeds after passing traffic-calming devices, although drivers did not reach the speed values observed before encountering them. In this context, Pérez-Acebo et al. [28] also recommended adopting specific spacing values for these devices in relation to vehicle speeds.

The effects of speed reduction are crucial in determining the performance and energy efficiency of TCMs; indeed, not all of these measures achieve the expected success. Some studies have shown that in 30 km/h zones located in an Italian city, motorcycles exhibited significant variations in speeds under high traffic volumes, while heavy vehicles and cars demonstrated only minor changes in speed [29]. The effectiveness of Zone 30 was also examined by [30], whose results indicated that some TCMs had no impact on road capacity. García et al. [31] conducted a micro-simulation study to compare different types and spacings of traffic-calming devices. They demonstrated that speed tables and speed humps did not affect capacity, where the slope of the entry ramp was less than 5%. On the other hand, Shirmohammadi et al. [32] used Aimsun to assess the effect of TCMs and their mutual positioning in the network on roadway capacity. The authors found that TCMs improved design quality and had a direct impact on network capacity, although this could change with variations in the number and location of TMCs in the road network.

Furthermore, TCMs have an impact on vehicular emissions and energy efficiency, with the extent of influence varying depending on the specific devices implemented. According to [33,34], speed bumps have been found to increase the generation of pollutants. Similarly, trapezoid-shaped speed humps made of asphalt and plastic, as well as circular speed bumps, were associated with higher vehicular emissions [35]. Ghafghazi and Hatzopoulou [36] used traffic simulation and microscopic emission modeling to demonstrate that the application of TCMs, whether as isolated measures or as part of area-wide patterns, resulted in increased air emissions. In particular, isolated TMCs, on average, led to a 1.5% increase in carbon dioxide emissions, a 0.3% increase in carbon monoxide emissions, and a 1.5% increase in nitrogen oxides emissions. Conversely, area-wide patterns were associated with a more substantial increase, including a 3.8% rise in carbon dioxide emissions, a 1.2% increase in carbon monoxide emissions, and a 2.2% increase in nitrogen oxides emissions at the network level. Simulations conducted along corridors showed emissions increasing by up to 83%.

One of the side effects of reducing vehicle speeds through traffic-calming measures is the potential reduction in traffic noise levels [37,38]. Vehicles traveling at lower speeds tend to generate less noise compared to when they are moving at higher speeds [39]. Moreover, certain traffic-calming measures, such as road surface modifications, vertical traffic-calming devices, or noise barriers, can directly target and mitigate traffic noise over time [38]. El-Bardisy et al. [39] suggested that urban designers should incorporate noise prediction into various stages of the design process to ensure that outdoor spaces are functional as well as aesthetically pleasing and meet the needs of the road user community. Concerning roundabouts used as TCMs, their geometric design should be meticulously studied during the preliminary design phase. Proper modeling is essential to optimize their potential for reducing traffic noise levels [4,37]. Nonetheless, the efficiency of noise reduction achieved by TCMs depends on several factors, including the type of road signaling used, the composition of traffic flow, the driving behavior of road users, as well as the type of device deployed and its placement along the road network [38]. In this way, TCMs also have the potential to enhance the quality of life and well-being of citizens in urban centers. However, these devices and measures have been in place for some time, especially in northern European cities. Despite the numerous benefits of TCMs [4,40,41], the question of whether their traffic-calming effects will endure over time remains open.

In the process of urban technological transition, the digitization of traffic-calming devices and the analysis of their interaction with modern intelligent transport systems cannot be overlooked. Considering one of the most popular technological innovations in the automotive field, namely CAVs, it would be interesting to comprehend their behavior when encountering TCMs and the potential benefits they could bring or integrate [42,43]. CAVs offer similar advantages to TCMs, such as reduced traffic delay, congestion, travel costs, and consequently, energy consumption, thereby providing several benefits for the urban environment and road users [42,44]. Additionally, CAVs have the potential to enhance accessibility, promote sustainable mobility, increase network capacity, and improve traffic safety and energy savings (e.g., [45–47]). While numerous studies have focused on the separate benefits, efficiency, and potential of TCMs and CDTs, there is currently a research gap regarding the effects of their combination [48]. Furthermore, since CAVs have not yet been fully introduced to the market, their driving behavior in the presence of TCMs is not well understood.

Building upon the above, this research can contribute to understanding how connected and automated technologies can be effectively integrated with TCMs, leading to new insights and knowledge in the field. Additionally, this research can provide data-driven analysis to validate the effectiveness of incorporating CAV technologies in improving operational and energy efficiency as well as the safety performance of TMCs. This can help to have a scientific approach for understanding the benefits and impacts of these technologies on traffic management. From a societal perspective, the research can contribute to enhanced urban mobility and improve overall safety. The integration of connected and automated technologies with traffic-calming measures can assist in reducing fuel consumption, emissions, and energy waste, ultimately leading to a more environmentally friendly transportation system. Furthermore, the research findings can provide valuable insights to urban planners and policymakers regarding the advantages and challenges associated with incorporating connected and automated technologies with TCMs. This, in turn, can guide the development of appropriate regulations and guidelines to support the integration of these technologies into urban planning and transportation policies.

3. Materials and Method

3.1. The Background of the Case Study

The study area is located along the coastline of Mazara del Vallo, Italy, a tourist-oriented town situated in southwestern Sicily. A segment of the road network approximately 1.9 km in length within this area, near the Fata Morgana seafront (latitude 37.663397° and longitude 12.556683°), was redesigned (see Figure 2). This redesign was part of a broader mobility project aimed at planning the future development of a city itinerary along the seashore. The current road platform has a width of 9.75 m, with two traffic lanes (one for each direction) and a sidewalk on the side facing the sea, which also allows parallel parking. During the summer season, a temporary roundabout is set up at the intersection with Del Mare Street (as shown in Figure 2), and the road is converted into one-way traffic. This change results in the westbound traffic lane being transformed into a one-lane cycle path.

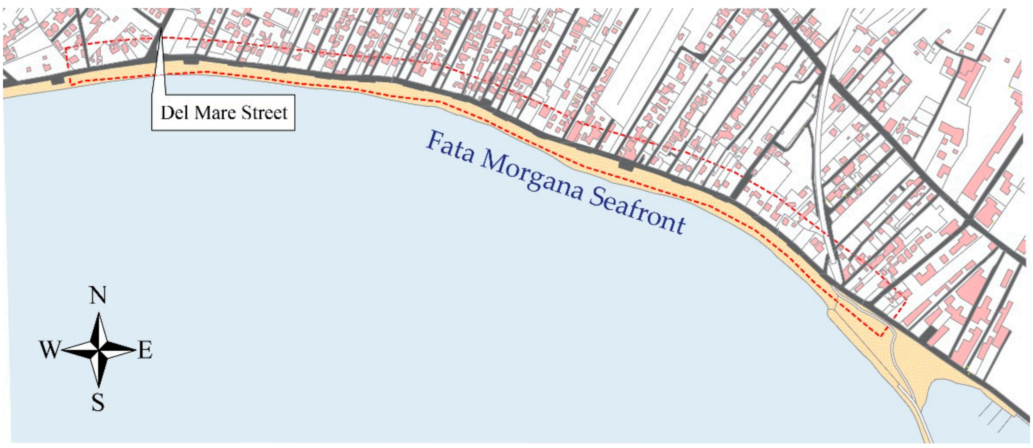

Figure 2. The study area with the red hatched zone enclosing the redesigned road network.

Figure 3 shows the current layout of the road network under examination, which serves as the baseline for comparing the three designed solutions that are conceptualized and described in the following sections.

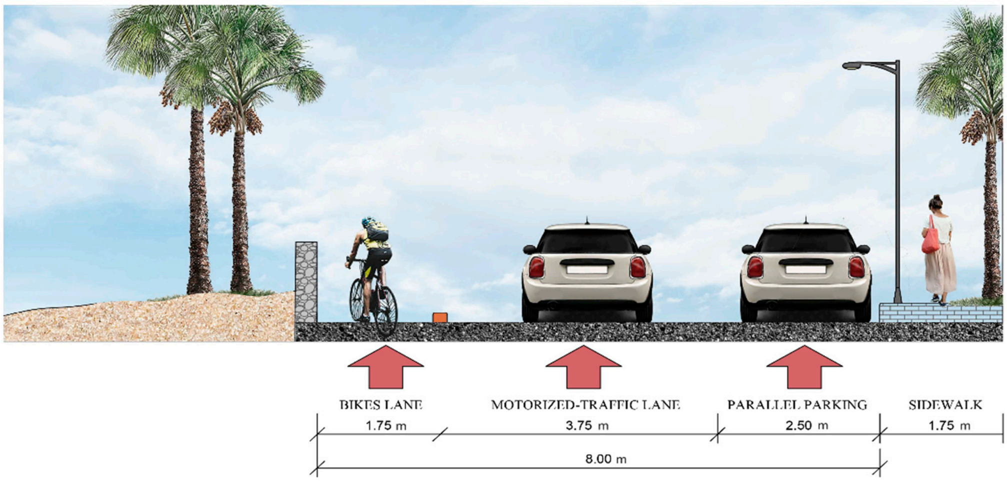

Figure 3. The road cross-section of the base layout. Note that the red arrows indicate the direction of travel, and all measures are expressed in meters (m).

The road network model was constructed in Aimsun Next to simulate various traffic patterns and evaluate the operational performance of CAVs used as a collective mobility service in the examined urban area where TCMs were designed (as discussed in Section 3.3). The planned TCMs in the road network involved the installation of a new east roundabout, referred to as R1, the establishment of a Limited Traffic Zone (LTZ), and the completion of the existing roundabout, referred to as R2, which is located in the western part of the network between Del Mare Street and the Fata Morgana seafront (as shown in Figure 4). According to [49], both intersections designed here can be categorized as mini roundabouts; however, roundabouts employed as TCMs can take on various designs depending on the specific characteristics of the urban area where they are intended for speed moderation [12]. The single-lane four-legged roundabout, R1, has an outer diameter of 21 m and features one-way entry and exit lanes on each approach. The single-lane three-legged roundabout, R2, has an outer diameter of 18 m with one-way entry and exit lanes on each approach. The entry and exit lane widths varied in the three designed solutions proposed here [49]. Both roundabouts have a six-meter-wide circulatory roadway and a partially surmountable central island to facilitate the maneuvers of larger vehicles, such as the CAVs used in the public transport system [4]. The deflection angles of both roundabouts meet the requirements specified by [49].

Figure 4. The road network built in Aimsun Next with the two roundabouts designed as TCMs. Note that TCMs stand for traffic-calming measures.

Figure 4 displays the road network constructed in Aimsun Next, providing a visual representation of the locations of the two roundabouts. This figure also illustrates the placement of the public transport service terminal within the road network. On the other hand, Figure 5 illustrates the geometric characteristics of each roundabout, as modeled in Aimsun.

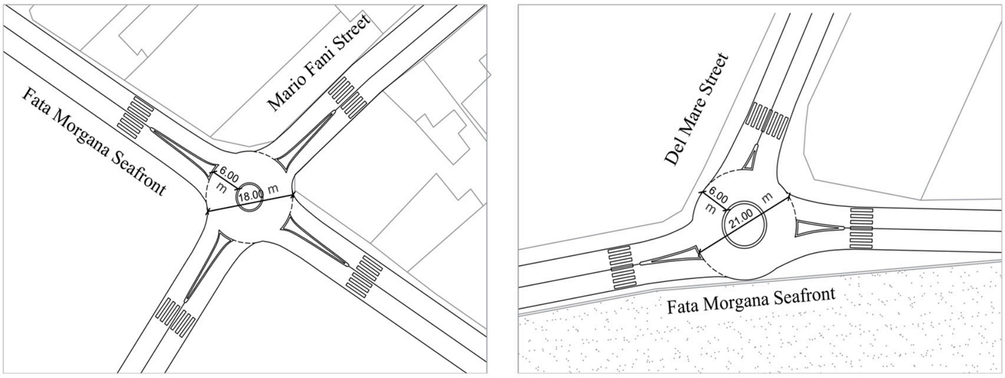

(**a**) (**b**)

Figure 5. Schemes of roundabouts are listed as: (**a**) The R1′s geometry; (**b**) The R2′s geometry. Note that all measures are expressed in meters (m).

To structure two plausible traffic scenarios reflecting real-world conditions, a data survey was conducted in the field through both manual observations and videotaping. The survey was carried out in an intermediate section of the network under study during peak hours, specifically from 1:00 p.m. to 2:00 p.m. on weekdays in April and May of 2023. An overall entry flow of 680 vehicles per hour was recorded with motorcycles accounting for approximately 12% of the total vehicles. The presence of heavy vehicles was negligible, considering that heavy traffic was redirected away from the Fata Morgana seafront due to an overpass at the entrance of the road network. Additionally, as the survey took place before the start of the tourist season, pedestrian traffic through the road network was estimated at approximately 7%. Notably, the existing road layout did not include a designated cycle path, resulting in an approximate flow of 10 bicycles per hour. During the tourist season, especially in the summer, this seaside resort experiences a significant increase in movements to and from the area. This period is characterized by intense pedestrian activity, accounting for approximately 40% of all traffic through the site, as it is one of the most frequented beaches by the local population in Mazara Del Vallo. With the aim of promoting more sustainable mobility along the seafront, the LTZ was introduced to restrict access for heavy vehicles and limit the entry of HOVs during specific time slots. Consequently, the distribution of traffic lanes and their widths on the current road platform was redesigned, considering three alternative Project Solutions (referred to as PS1, PS2, and PS3), as illustrated in Figure 6. PS1 and PS3 (as seen in Figure 6a,c) both involve the removal of streetside parallel parking. In contrast, PS2 includes reserved parallel parking exclusively for residents, which was located along the seafront between consecutive bus stops (as depicted in Figure 6b). To accommodate the parking demand, several parking areas were established throughout the road network under examination.

In Figure 6a, PS1 is depicted, where the public transport service follows a circular route starting from the terminal near R1 (as shown in Figure 4). It proceeds along a dedicated lane to reach R2, crosses it, and then enters a shared lane with HOVs before returning to the terminal. Figure 6b and Figure 6c illustrate PS2 and PS3, respectively. In PS2, CAVs and HOVs share the same traffic lane in the east–west direction, excluding heavy vehicles and other motorized traffic. In contrast, in PS3, CAVs have their dedicated lane within the road network. All three design solutions incorporate dedicated cycle paths. In PS1 and PS3, the cycle paths are designed as one-way lanes for bicycles, while in PS2, the bike path consists of two lanes, each designated for travel in a specific direction.

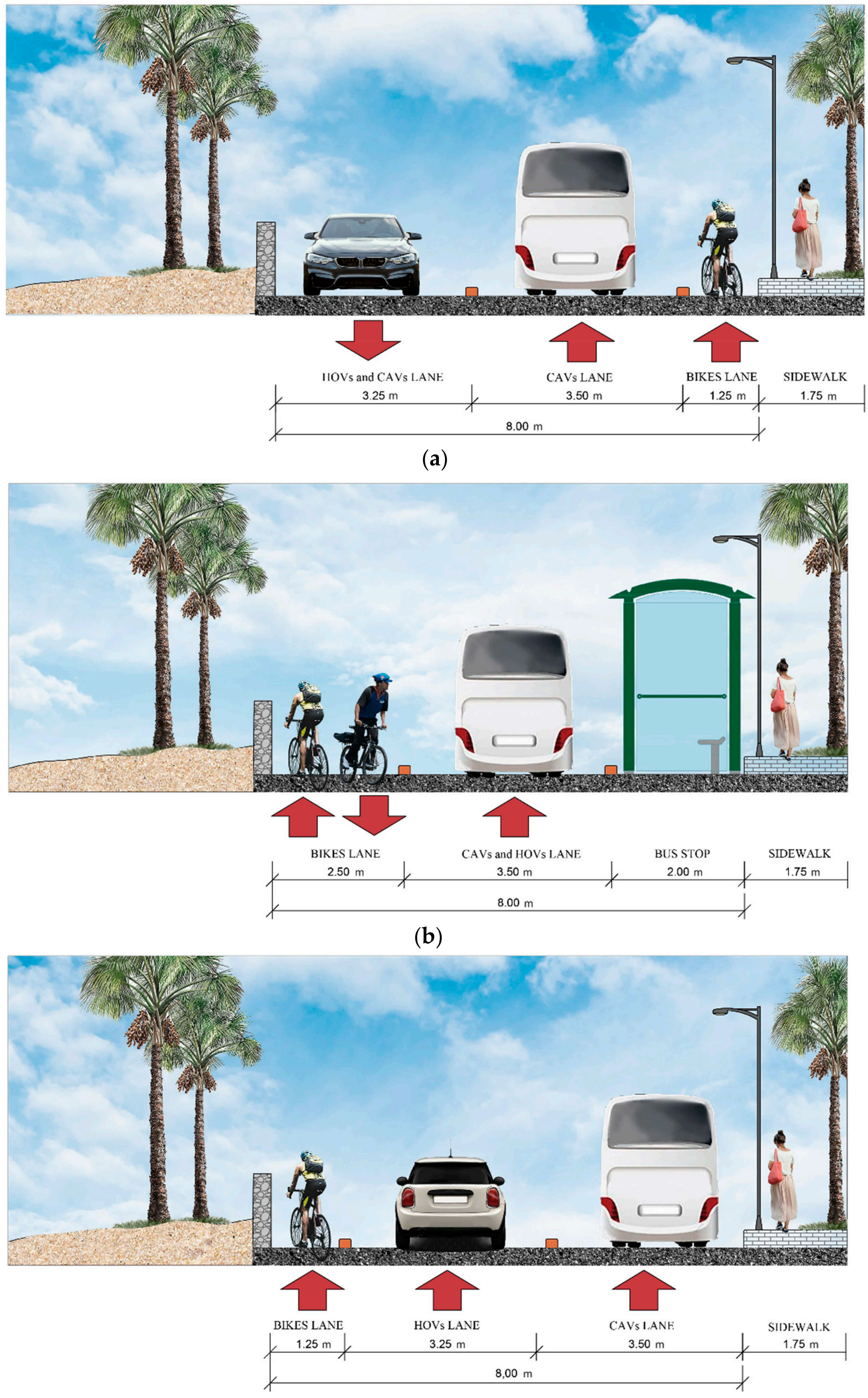

Figure 6. The road cross-section of the planned network related to the project solutions: (**a**) the project solution 1 (PS1); (**b**) the project solution 2 (PS2); (**c**) the project solution 3 (PS3). Note: CAVs stand for connected and automated vehicles; HOVs stand for human-operated vehicles; the red arrows indicate the direction of travel, and all measures are expressed in meters (m).

3.2. The Simulation Plan

As for the conceptualized TCMs strategy, the LTZ is planned to be active every day of the week, from June to September for a duration of ten hours each day. More precisely, the LTZ is scheduled to operate from 9:00 a.m. to 7:00 p.m. and is divided into the following time slots:

- Time Slot 1 (TS1): This time slot spans from 9:00 a.m. to 1:00 p.m., and within this timeframe, access to the LTZ is restricted for all motorized traffic except for CAVs used as part of the public mobility service. In other words, regular vehicles are not permitted during this period, but autonomous vehicles providing mobility services can still operate.
- Time Slot 2 (TS2): This time slot spans from 1:00 p.m. to 4:00 p.m., allowing access for all categories of traffic. This means that all vehicles, including regular cars, are permitted to enter the LTZ during this period. This time interval offers flexibility for residents who may need to return home for lunch and then travel back to work as well as for others who need to move in and out of the area.
- Time Slot 3 (TS3): This time slot extends from 4:00 p.m. to 7:00 p.m. It is similar to TS1, as access to the LTZ is restricted for all motorized traffic except for CAVs. Similar to the morning time slot, only autonomous vehicles used for mobility services are allowed during TS3.

To account for various traffic patterns, the three Project Solutions (i.e., PS1, PS2, PS3) were simulated in Aimsun Next, considering two alternative traffic scenarios: Traffic Scenario A (TSA) and Traffic Scenario B (TSB). These scenarios were distinguished by the traffic flows of each user type during the proposed time slots. Each scenario was divided into three subsequent time slots, each associated with the operation of the LTZ. Furthermore, to assess the overall energy performance of the design solutions for TCMs featuring CDTs, traffic throughputs simulated for each designed scenario were compared to the baseline traffic scenario, which included the base layout and a specified traffic composition. This approach enabled a comparison of each designed project solution with the actual conditions.

The organization of the simulation plan by project solution and traffic scenario is summarized in Table 1. Then, Table 2 presents the composition of traffic flows for the simulated traffic scenarios A and B broken down by time slot. Additionally, Table 3 delineates the simulated baseline traffic scenario, which is divided into two cases (i.e., baseline traffic scenarios A and B), where each traffic composition corresponds to traffic flows simulated in TSA or TSB during TS2. To facilitate the comparison among the three design solutions and the base layout, the traffic flow composition planned for TS2 in TSA is identical to BTSA. Similarly, the traffic flows in TS2 for TSB are identical to BTSB (see Tables 2 and 3).

Table 1. The organization of the simulation plan.

Project Solution 1 (PS1)	
Traffic Scenario A (TSA) Time Slot 1 (9:00 a.m.–1:00 p.m.) Time Slot 2 (1:00 p.m.–4:00 p.m.) Time Slot 3 (4:00 p.m.–7:00 p.m.)	Traffic Scenario B (TSB) Time Slot 1 (9:00 p.m.–1:00 p.m.) Time Slot 2 (1:00 p.m.–4:00 p.m.) Time Slot 3 (4:00 p.m.–7:00 p.m.)
Project Solution 2 (PS2)	
Traffic Scenario A (TSA) Time Slot 1 (9:00 a.m.–1:00 p.m.) Time Slot 2 (1:00 p.m.–4:00 p.m.) Time Slot 3 (4:00 p.m.–7:00 p.m.)	Traffic Scenario B (TSB) Time Slot 1 (9:00 a.m.–1:00 p.m.) Time Slot 2 (1:00 p.m.–4:00 p.m.) Time Slot 3 (4:00 p.m.–7:00 p.m.)
Project Solution 3 (PS3)	
Traffic Scenario A (TSA) Time Slot 1 (9:00 a.m.–1:00 p.m.) Time Slot 2 (1:00 p.m.–4:00 p.m.) Time Slot 3 (4:00 p.m.–7:00 p.m.)	Traffic Scenario B (TSB) Time Slot 1 (9:00 a.m.–1:00 p.m.) Time Slot 2 (1:00 p.m.–4:00 p.m.) Time Slot 3 (4:00 p.m.–7:00 p.m.)
Base Layout (BL)	
Baseline Traffic Scenario A (BTSA)	Baseline Traffic Scenario B (BTSB)

Table 2. The simulated traffic scenarios A and B. Note that HOVs stands for human-operated vehicles; CAVs stands for connected and automated vehicles.

Traffic Scenario A (TSA)		
Time Slot 1	Time Slot 2	Time Slot 3
Bike: 80/120/160/200 bike/h Shuttle bus (CAV) frequency: 15′ HOVs: no vehicle Pedestrian flow: 200 ped/h	Bike: 120 bike/h Shuttle bus (CAV) frequency: 15′ HOVs: 750/600/750 veh/h Pedestrian flow: 150 ped/h	Bike: 140/160/180 bike/h Shuttle bus (CAV) frequency: 15′ HOVs: no vehicle Pedestrian flow: 220 ped/h
Traffic Scenario B (TSB)		
Time Slot 1	Time Slot 2	Time Slot 3
Bike: 120/160/200/240 bike/h Shuttle bus (CAV) frequency: 10′ HOVs: no vehicle Pedestrian flow: 220 ped/h	Bike: 160 bike/h Shuttle bus (CAV) frequency: 10′ HOVs: 1000/850/1000 veh/h Pedestrian flow: 200 ped/h	Bike: 160/180/200 bike/h Shuttle bus (CAV) frequency: 10′ HOVs: no vehicle Pedestrian flow: 220 ped/h

Table 3. The simulated baseline traffic scenarios A and B. Note that HOVs stand for human-operated vehicles.

Baseline Traffic Scenario A (BTSA)	Baseline Traffic Scenario B (BTSB)
Bike: 120 bike/h HOVs: 750/600/750 veh/h Pedestrian flow: 150 ped/h	Bike: 160 bike/h HOVs: 1000/850/1000 veh/h Pedestrian flow: 200 ped/h

3.3. Aimsun Next Modeling

Aimsun Next was used to simulate the traffic flows of all road users considered for this case study [9]. The movement of vehicles simulated microscopically is updated for each simulation step and is governed by a series of algorithms. One of these algorithms is the arrivals algorithm, which controls when the traffic flows defined in the Origin–Destination (OD) matrix, or alternatively in the Traffic State, can enter the network with a certain headway between vehicles. As vehicles traverse the network, they are updated based on vehicle behavioral models, namely the "Car-Following" and "Lane-Changing" models [50–52]. These models operate on the assumption that drivers will travel at their desired speed when not influenced by the surrounding traffic environment. However, their driving behavior is influenced by interactions with other road users, speed limits imposed, and traffic control signals.

For this case study, only the "Car-Following" model was employed, since lane changes were prevented by the geometric layout of the examined road network. Additionally, the Adaptive Cruise Control (ACC) and Cooperative Adaptive Cruise Control (CACC) modules were used to simulate the CDTs. These modules control speeds based on the presence of a leading vehicle, if any [9,50]. In accordance with the assumptions that underlie the simulation of CDTs [50], CAVs equipped with the CACC system were enabled for vehicle-to-vehicle communication to negotiate the right of way at any intersections when they encounter another cooperative driver. Alternatively, when CAVs approached intersections and encountered non-cooperative HOVs, they could activate the ACC. The yielding behavior of drivers at intersections is simulated in Aimsun Next using the Gap Acceptance model [41]. By evaluating a range of parameters for each vehicle approaching the intersection, this model determines whether a vehicle can enter the intersection in accordance with priority rules. This model employs a decision-making process by assessing potential conflicts, calculating the relative distance between vehicles, and considering their speeds, acceleration rates, and the time required for the vehicles to clear the intersection [9].

In accordance with each scenario, the Origin–Destination (OD) matrix for all user classes, except for CAVs, was created in Aimsun Next. Since CAVs were used as a public transportation system, their traffic flows were simulated by establishing a timetable and using reserved lanes with dedicated stops for passengers. To facilitate this, public transport plans were devised, encompassing public transport routes (see Figures 6–8). In alignment with the organization of the simulation plan outlined in Table 1, and the traffic composition of the simulated traffic scenarios in Tables 2 and 3, a set of timetables was devised to govern the departure frequency. The public transport service was operated by autonomous and connected bus shuttles. Each CAV used for the public transport service was appropriately designed with dimensions of 6.5 m in length, 2.25 m in width, a maximum capacity of 20 passengers, and a maximum cruising speed of 25 km/h. Moreover, in line with the assumed driving behavior of CAVs, 100% of them were equipped with Cooperative Adaptive Cruise Control (CACC) devices [43,50]. The necessary vehicle-to-vehicle communication capabilities were assumed to be in place with a high degree of reliability [50].

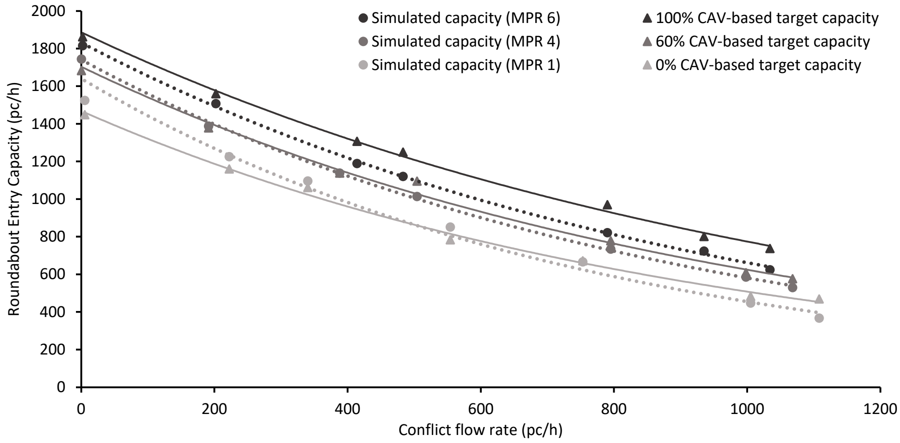

Figure 7. Simulated roundabout capacity compared with capacity target curves. Note that MPR 1, MPR 4, and MPR 6 stand for the Market Penetration Rates of 0% CAVs, 60% CAVs, and 100% CAVs respectively, and CAVs stand for connected and automated vehicles.

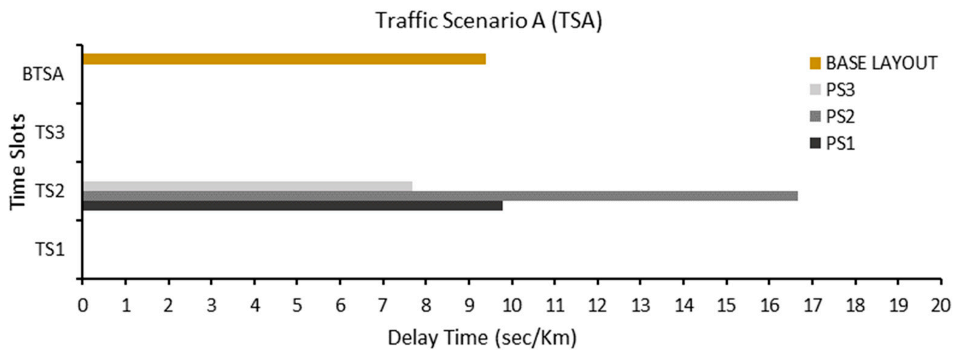

(**a**)

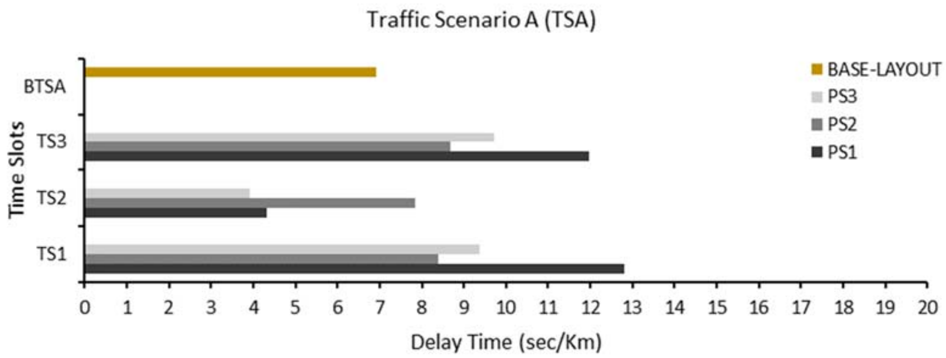

(**b**)

Figure 8. *Cont.*

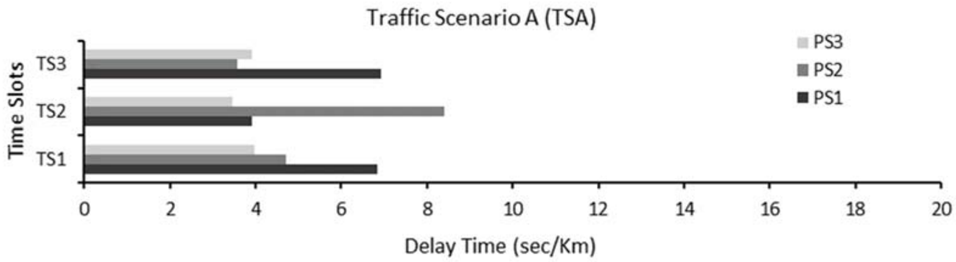

(**c**)

Figure 8. Delay time values in seconds returned by Aimsun in the Traffic Scenario A (TSA) with reference to different users 'classes: (**a**) HOVs; (**b**) bikes; (**c**) shuttle buses. Note that PS1, PS2, and PS3 are Project Solutions 1, 2, and 3, respectively; BTSA stands for the baseline traffic scenario A; TS1, TS2, and TS3 stand for Time Slots 1, 2, and 3, respectively; HOVs stand for human-operated vehicles; CAVs stand for connected and automated vehicles.

Before initiating the calibration process, the capability of Aimsun Next to replicate the observed traffic flows (as described in the previous section) was assessed. To achieve this, the observed flow matrix was simulated for a duration of 60 min, including a 15-min initialization period required to load the traffic into the network and attain equilibrium conditions. Since the Geoffrey E. Havers (GEH) statistic, calculated by comparing the simulated flow rates with the observed data, was found to be less than five for over 96% of the cases, we proceeded to the subsequent step involving the calibration process [51].

Different market penetration rates (MPRs) of CAVs in the traffic stream were set as follows: MPR (1) 0% CAVs; MPR (2) 20% CAVs; MPR (3) 40% CAVs; MPR (4) 60% CAVs; MPR (5) 80% CAVs; MPR (6) 100% CAVs. According to [6], the traffic demand data were divided into two Origin–Destination (O/D) matrices, each with an MPR of CAVs, and the remaining (1-MPR) consisted of HOVs.

To account for the presence of CAVs on the roundabouts in Figure 5, the target capacity curves were constructed using a general formula that is valid for both single-lane and multi-lane roundabouts, as follows [50,51]:

$$C_{e,adj,CAVs} = f_A \cdot A \cdot e^{-f_B \cdot B \cdot Q_c} \quad (1)$$

where $C_{e,adj,CAVs}$ represents the entry lane's CAV capacity (vehicles per hour), A defines the intercept parameter, and B defines the slope parameter. Capacity is determined by the distribution of gaps in the circulating traffic flow, the decision-making process of drivers regarding the acceptance of these gaps for entering the roundabout, and the follow-up headways required by each driver in a queue. According to [50], for roundabouts with one-lane entry conflicted by one circulating lane, a value of 1380 was adopted for A. This value was calibrated using a follow-up headway of 2.61 s, which is consistent with the observed value in the field on similarly-sized roundabouts in Mazara Del Vallo. In turn, the value of 1.02×10^{-3} was adopted for B, which corresponds to the field-measured value for a critical headway of 4.9 s [50]. The adjustment factors, f_A and f_B, are employed to modify the intercept and slope parameters, respectively. These adjustment factors assume different values based on the roundabout layout and the penetration rates of CAVs [50]. The adjustment factor for the intercept parameter (f_A) is set to 1.00 when there are no CAVs (0%) in the traffic, and all vehicles are HOVs. Its value increases as the CAV penetration rate rises [50]. The adjustment factor for the slope parameter (f_B) is 1.00 when the percentage of HOVs in traffic is 100%. Its value decreases as the CAV penetration rate increases [50]. Following the approach outlined in [6], capacity target curves were developed for market penetration rates of CAVs in traffic ranging from 0% to 100% with increments of 20%. These curves were used to compare the roundabout capacity data simulated in Aimsun Next for calibration purposes. To simulate traffic from free-flowing conditions to capacity, six subsequent Origin–Destination matrices were assigned to the respective entry lane. This ensured that the entering traffic flow reached saturation, with circulating traffic increasing from 0 to 1200 vehicles per hour in increments of 200 vehicles per hour. A 10-min warm-up time was initially allocated to load traffic flows into the road network. Simulation from free-flowing to capacity was initiated so that the number of vehicles expected to enter the roundabout aligned with the entry capacity values recorded by detectors on the network model of each roundabout.

There was a need to calibrate the model to characterize the driving behavior of CAVs and HOVs on the roundabout network models where there is more significant interaction between vehicular trajectories due to turning movements. To achieve this, the model parameters were fine-tuned by comparing the simulated capacity values with the target capacity curves, as introduced in the previous section. Applying a sensitivity analysis, it was determined that the model parameters affecting HOVs' driving behavior were the speed limit acceptance, gap, and reaction time [9]. The speed acceptance parameter represents the driver's attitude toward speed limits. A value greater than 1 indicates that the vehicle will use speeds higher than the speed limit, while a value lower than 1 means the vehicle will adhere to speeds lower than the speed limit. The gap parameter measures the headway between vehicles, which was calculated from the front bumper of the leading vehicle to the front bumper of the following vehicle [9].

In turn, the reaction time represents the duration it takes for a driver to respond to changes in the speed of the preceding vehicle. This parameter can be configured as "fixed", where it remains the same for all vehicle classes on the road network and equals the simulation step, or as "variable", which is a multiple of the simulation step [9]. The reaction time has a notable impact on section capacity; a lower reaction time results in higher road capacities because drivers can maintain closer distances to the preceding vehicle and identify gaps more readily to enter the network. Furthermore, for modeling CAVs in traffic, specific model parameters included the maximum acceleration, which is defined in Gipps's car-following model [51,52] and represents the maximum acceleration a vehicle can achieve under any circumstances. Additionally, there was the safety margin factor, which determined when a vehicle could proceed at a priority junction and provided a multiplier for the safety margin values [9].

Table 4 presents both the default and simulated values of these vehicle parameters as a result of the fine-tuning process conducted in Aimsun. The model parameters obtained in this manner for roundabouts R1 and R2 were then applied to simulate the entire road network under examination.

Table 4. Results of the fine-tuned parameter process for the one-lane roundabouts under study. Note that HOVs stand for human-operated vehicles; CAVs stand for connected and automated vehicles.

Parameter	Default Value	Calibrated Value
	HOVs	
Reaction time [1] (s)	0.80	0.86
Speed limit acceptance	1.10	1.00
Gap (s)	0.00	1.58
	CAVs	
Reaction time [1] (s)	0.80	0.63
Maximum acceleration (m/s^2)	3.00	4.00
Safety margin factor	1.00	0.50

[1] The value of the reaction time under mixed traffic is the weighted average of the parameter value for each vehicle class, where the weights are the percentages of CAVs or HOVs by scenario.

By way of example, Figure 7 illustrates the target capacity curves alongside the simulated capacity data for different market penetration rates (MPRs) of CAVs, specifically for MPRs of 0%, 60%, and 100%.

Table 5 presents the measures of goodness of fit that were employed to validate the fine-tuning process of the model parameters. The table includes values for several metrics, including the root mean squared normalized error (RMSNE), which provides information about the magnitude of errors concerning the average measurement; Theil's indicator (U), a normalized measure of relative error that helps smooth out the impact of large errors; and the Geoffrey E. Havers' statistic (GEH) [51]. The GEH statistic calculates an index for each counting station and assists in confirming the model's accuracy by ensuring that the deviation of the simulated values from the measurements is smaller than 5% in at least 85% of the cases [51].

Table 5. Statistics for entry lane capacity target values and simulated data. Note that CAVs stand for connected and automated vehicles.

	Market Penetration Rate of CAVs (%)					
	0	**20**	**40**	**60**	**80**	**100**
$RMSNE = \sqrt{\frac{1}{N}\sum_{i=1}^{N}\left(\frac{x_i-y_i}{y_i}\right)^2}$	0.12	0.11	0.08	0.07	0.09	0.11
$U = \frac{\sqrt{\frac{1}{N}\sum_{i=1}^{N}(x_i-y_i)^2}}{\sqrt{\frac{1}{N}\sum_{i=1}^{N}(x_i)^2}+\sqrt{\frac{1}{N}\sum_{i=1}^{N}(y_i)^2}}$	0.04	0.04	0.03	0.02	0.03	0.04
$GEH_i = \sqrt{\frac{2(x_i-y_i)^2}{x_i+y_i}}$	93.00	93.00	100.00	100.00	96.00	93.00

RMSNE is the normalized root mean square error, U is Theil's indicator, and GEH is the Georey E. Havers' statistic where N means the number of observations, while x_i and y_i are the simulated value and the corresponding target capacity value [51].

The environmental impact of the three design solutions was also assessed using simulation, as detailed in reference [53]. Given that the shuttle buses operate on a fully electric power supply, pollution emissions of carbon dioxide (CO_2) and oxides of nitrogen (NOx) were estimated for HOVs only. This estimation was carried out using a specific environmental model within Aimsun. To achieve this, the London Emissions Model, as implemented by [9], was employed. It took into account the proportion of HOVs with their respective fuel types and Euro-class emission standards as input data.

Since pedestrians are the most vulnerable road users, evaluating pedestrian flows and their interactions with other traffic components is crucial for assessing the safety of urban road spaces. To incorporate pedestrians into the simulated network, a pedestrian area was designated, featuring crosswalks as well as pedestrian entry and exit points. Following the simulation plans outlined here (see Table 1), pedestrian flows were simulated by creating a dedicated OD matrix. Consequently, all types of road users permitted within the road network were simulated within the Aimsun Next Dynamic Scenario folder, which also included traffic demand data and the public transport plan.

To evaluate the safety performance of CAVs in conjunction with TCMs, trajectory files generated by Aimsun Next were analyzed using the Surrogate Safety Assessment Model (SSAM) software (version 3.0) developed by [10]. The SSAM software enables the assessment of the safety of various road facilities by computing several surrogate safety measures, including time to collision (TTC), post-encroachment time (PET), maximum speed (MaxS), delta-speed (DeltaS), deceleration rate (DR), and maximum deceleration (MaxD). The TTC parameter represents the minimum time-to-collision value observed during a conflict. According to the SSAM logic, a conflict event occurs when the TTC value reaches a critical threshold. The PET measures the time elapsed between the passage of the first vehicle and the second vehicle at the same location within the conflict area. Both TTC and PET serve as indicators of collision likelihood with smaller values indicating a higher probability of collision. The default values for TTC and PET are 1.5 s and 5.0 s, respectively. MaxS signifies the maximum speed of any vehicle involved in the collision, while MaxD corresponds to the maximum deceleration observed in the second vehicle during the conflict. DeltaS represents the difference in speed between two successive vehicles, and DR is the deceleration rate of the second vehicle recorded during the conflict event.

To ensure that the safety analysis remains independent of the source of trajectory files, the threshold values for the SSAM parameters, which have a significant impact on the safety analysis, were determined through a comparative evaluation involving various micro-simulators [54]. Based on the findings from [55,56], two key SSAM parameters affecting the results were identified: TTC and PET. Additionally, MaxS was recognized as a parameter that influences the SSAM outputs. Consequently, the results of the comparative analysis indicated that the threshold values for TTC and PET should be set at 1.5 s and 2.5 s, respectively. The minimum threshold value for MaxS was established as 1.0 s. These threshold values were chosen to maintain consistency and reliability in the safety analysis across different simulation sources [54].

The SSAM classifies conflict types based on the directions of colliding path vehicles. The classification includes rear-end, crossing, and lane-changing conflicts. Specifically, conflicts are categorized based on the conflict angle, which is the angle formed by the directions of two vehicles during their conflict. The SSAM classifies conflicts as follows:

1. Rear-end conflicts: the conflict angle is between 0° and 30°.
2. Lane-changing conflicts: the conflict angle is between 30° and 85°.
3. Crossing conflicts: the conflict angle is greater than 85°.

The safety analysis of the three designed solutions, conducted using surrogate safety measures, allowed for the calculation of potential conflicts and their severity during the simulation.

4. Results

The microsimulation outputs were analyzed to evaluate the operational performances of the strategy that combines CDTs and TCMs, which aimed at transitioning toward energy-efficient mobility services for smart cities. The comparison between the three design solutions and the baseline configuration of the road network was conducted from the perspectives of operation, air quality, and safety. In this context, the simulated delay outputs for each vehicle class across all the designed project solutions were considered as a metric for assessing operational performance and its potential impact on enhancing energy efficiency in urban areas. Furthermore, the environmental impact, particularly in terms of air quality, was assessed by estimating emissions from mobile sources. Since CAVs operate with a fully electric power supply, the emissions estimation focused on HOVs for the three alternative design solutions proposed in this study.

Then, the safety performance of the designed alternatives was assessed using surrogate safety measures, which provided the number of potential conflicts classified by severity. The comparison between each design solution (refer to Figure 6) and the current road layout (refer to Figure 3) was conducted during TS2 (see Tables 2 and 3). This comparison was carried out in alignment with the principles of the TCM strategy, which restricts motorized traffic access during specific times. TS2 represents the period when motorized traffic was allowed into the LTZ.

Figure 8 illustrates the delays for different road user types, including bikes, HOVs, and shuttle buses, for all three designed project solutions as simulated in Traffic Scenario A. In Figure 8a, it is evident that the best performance in delay reduction for HOVs was observed in PS3, where each user class has a dedicated lane. Specifically, PS3 showed an 18% reduction in delay compared to the base layout. On the other hand, PS1 and PS2 exhibited increases in delay, approximately 4% and 75%, respectively, when compared to the base layout.

The delay performance of PS2 was twice that of PS3, while the delay in PS1 was 28% higher than that in PS3. In the case of PS2, as shown in Figure 6b, HOVs share the lane with shuttle buses and are compelled to queue behind the buses at every bus stop, resulting in increased travel delays for HOVs. Similar results were observed for bikes (refer to Figure 8b), where PS3 demonstrated the best performance during TS2 with a 43% reduction in delay compared to the base layout. Figure 8b highlights that PS3 consistently recorded the minimum delay values during TS2 when each design solution was compared with the base layout.

In comparison, when considering TS1 and TS3, the delay values simulated for both PS2 and PS3 were found to be comparable. As expected, Figure 8b also reveals that the delay values of each design solution decreased during TS2 compared to other time slots. According to the traffic scenarios (see Tables 2 and 3), bike traffic flows decreased from TS1 to TS2 and subsequently increased from TS2 to TS3.

Figure 8c illustrates that the delay values simulated for shuttle buses in each project solution varied only slightly across different time slots (see Tables 2 and 3). When considering the total delay values calculated for each design solution over the entire LTZ operating time, PS3 exhibited the smallest delay compared to the other project solutions. It is important to note that the lane dedicated to shuttle buses in PS1 is positioned in the middle of the roadway between the HOV-dedicated lane and the cycle path (see Figure 6a). Therefore, the road platform configuration of PS1 could lead to greater delays than the other design alternatives due to interferences among turning movements of vehicles entering or exiting the network (see Figure 6b,c). In the designed PS2, shuttle buses share the traffic lane with HOVs, which can lead to delays caused by interactions with other vehicles.

Figure 9 also highlights the design solution that minimized the total delay experienced by all classes of users throughout the entire LTZ operating time. This parameter was calculated by summing the delay values simulated for each vehicular class traveling through the network in each design solution during Traffic Scenario A over the entire LTZ operation. The same figure shows that PS3 recorded the smallest total delay value with a percentage reduction in delay of 26% and 28% compared to PS1 and PS2.

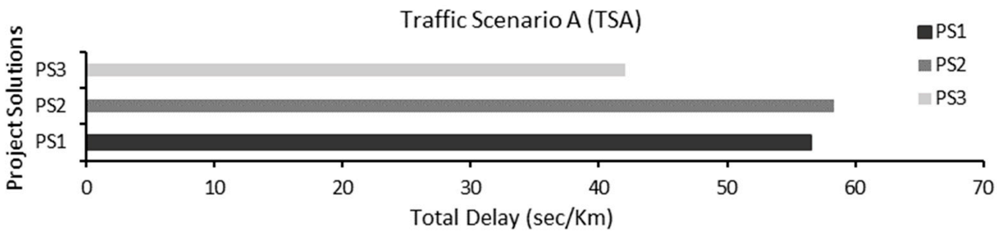

Figure 9. Total delay calculated for the simulation of the Traffic Scenario A (TSA) considering each vehicular class entering during the limited traffic zone (LTZ) operation time. Note that PS1, PS2, and PS3 are Project Solutions 1, 2, and 3, respectively.

Figure 10 displays the pollution emissions (specifically, CO_2 and NOx in grams) estimated for HOVs during the simulation of TS2 and BTSA. PS3 demonstrated a reduced environmental impact compared to PS1 and PS2 as well as the basic layout. PS3 achieved a 37% reduction in CO_2 emissions when compared to the base layout. In contrast, PS1 exhibited a 12% reduction in CO_2 emissions when compared to the base layout (see Figure 10a). From Figure 10a, we can observe a slight percentage increase in CO_2 emissions of around 3% when comparing PS2 with the simulated emission outputs of the base layout. Similar results were also found for NOx emissions. In light of this, the simulation results for TSA indicated that PS3 can enhance energy efficiency in terms of operational performance and air quality compared to the current conditions.

To account for various potential traffic scenarios that may manifest in the road network under study, the three design solutions were also simulated with a different traffic scenario, TSB, as presented in Table 2. Consequently, the delay performance experienced by each class of road users traveling the road network was evaluated in the three project solutions under examination, as depicted in Figures 11 and 12.

Specifically, Figure 11a illustrates the delay performance observed for HOVs in the three project solutions and the base layout during TS2. According to the planned LTZ, only HOVs are permitted to enter the network during TS2. Figure 11a clearly demonstrates that PS3 optimizes delay reduction compared to the other project solutions. The percentage reduction in delay achieved by PS3, in contrast to the base layout, is approximately 17%. When comparing the simulated delay values of PS1 and PS2 with the base solution (i.e., BTSB), there is an increase in delay by 13% and 67%, respectively. Additionally, the delay recorded in PS2 is approximately twice that of PS3, while the percentage reduction in delay achieved by PS3 is 26% compared to the delay experienced in PS1. The reduction in delay observed in PS3, as indicated by the simulated delay results for TSA, is likely attributable to the road platform's organization, where each class of road users has its own designated lane. This is in contrast to other design solutions where HOVs share traffic lanes with shuttle buses. Similar improvements in delay performance were also observed for bikes. When each project solution simulated during TS2 is compared with the base layout, bikes experience less delay in PS3 (refer to Figure 11b). In fact, the simulation of PS3 results in a percentage reduction in delay of approximately 30% compared to the base layout. Additionally, PS3 exhibits the lowest total simulated delay throughout the entire operation of the LTZ. Therefore, PS3 proves to be the most promising solution in terms of the operational performance of the studied road network for bikes. Also, the one-way cycle path along the waterfront, as designed in PS3, incurs fewer delays due to minimal interactions with traffic flows entering the network.

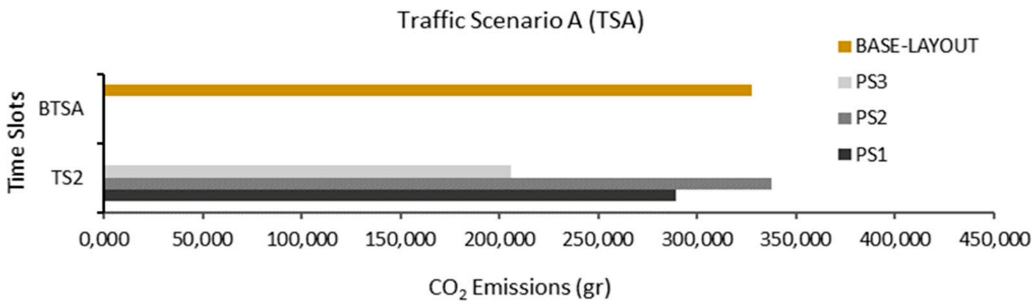

(**a**)

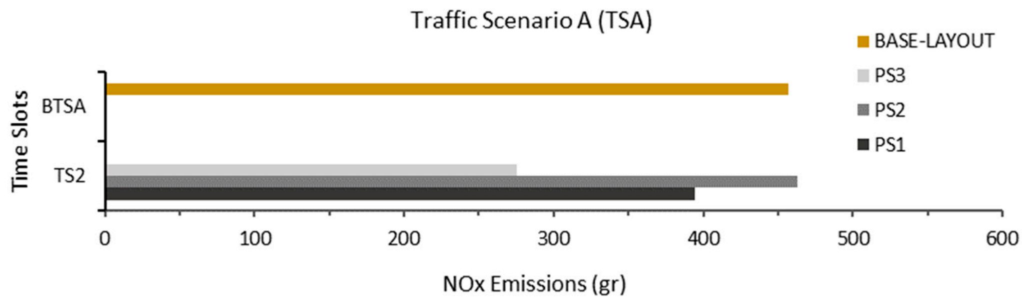

(**b**)

Figure 10. Simulated pollution emissions: (**a**) HOVs' CO_2 pollution values in grams returned by Aimsun in traffic scenario A (TSA); (**b**) HOVs' NOx pollution values in grams returned by Aimsun in traffic scenario A (TSA). Note that PS1, PS2, and PS3 are Project Solutions 1, 2, and 3, respectively; BTSA stands for baseline traffic scenario A; TS2 stands for Time Slot 2.

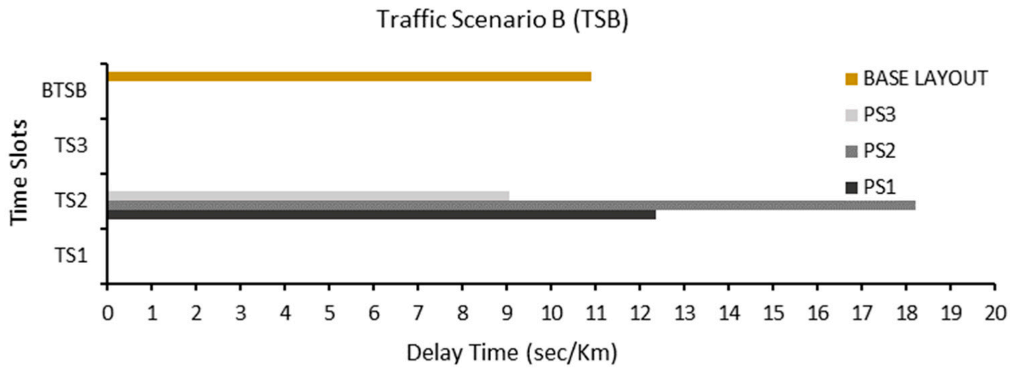

(**a**)

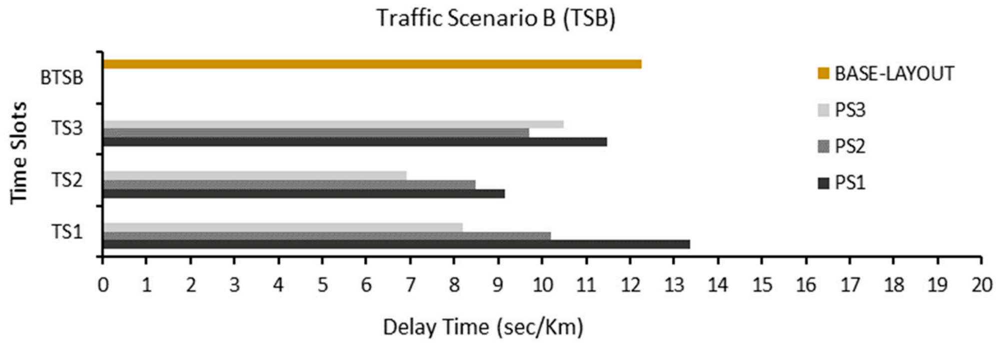

(**b**)

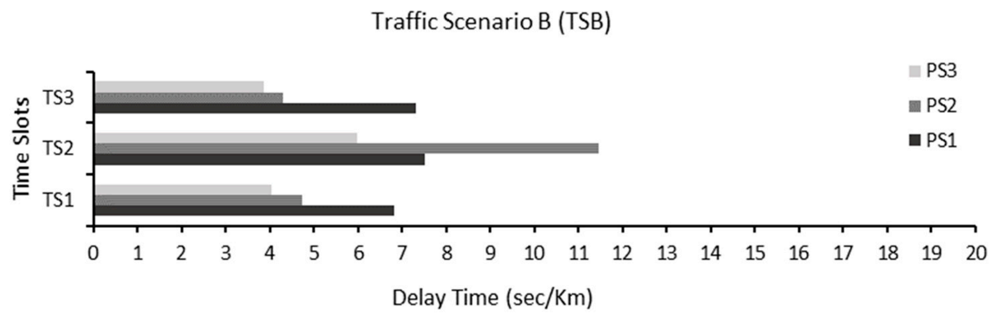

(**c**)

Figure 11. Delay time values in seconds returned by Aimsun in traffic scenario B (TSB) with reference to different users 'classes: (**a**) HOVs; (**b**) bikes; (**c**) shuttle buses. Note that PS1, PS2, and PS3 are Project Solutions 1, 2, and 3, respectively; BTSB stands for baseline traffic scenario B; TS1, TS2 and TS3 stand for Time Slots 1, 2, and 3, respectively; HOVs stand for human-operated vehicles; CAVs stand for connected and automated vehicles.

Comparing the delay performance of the three design solutions, Figure 11c demonstrates that the simulation of shuttle buses in PS3 yielded the lowest delay values during each time slot. Hence, as it was evident for PS3 under TSA (see Figure 6c), the placement of the reserved lane for shuttle buses near the sidewalk was once again the most effective design solution for minimizing travel delay. Figure 12 illustrates the total delay calculated for each design solution by summing the delay values recorded by each class of vehicles during the operation of the LTZ. Similar to TSA, in TSB, PS3 is the most operationally efficient solution, as it resulted in a lower total delay compared to the other design alternatives. Specifically, the percentage reduction in delay for PS3 respect to PS1 and PS2, was approximately 28% and 29%, respectively.

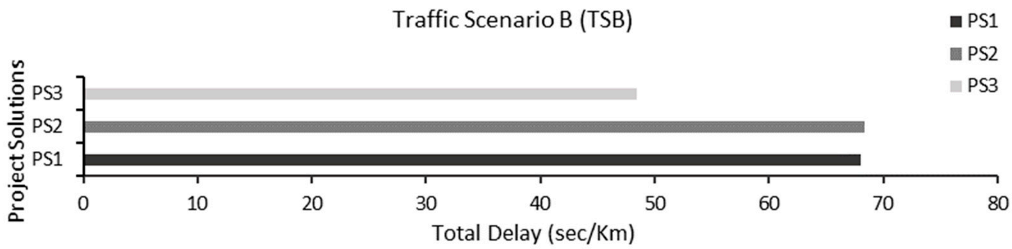

Figure 12. Total delay calculated for the simulation of the traffic scenario B (TSB) considering each vehicular class entering during the Limited Traffic Zone (LTZ) operation time. Note that PS1, PS2, and PS3 are Project Solutions 1, 2, and 3, respectively.

The environmental impact of the three design solutions was also evaluated by analyzing the estimated emissions of pollutants during the simulation of HOVs. Figure 13 displays the emissions of CO_2 and NOx in grams produced during the three hours of simulation conducted under TS2 and BTSB (refer to Tables 2 and 3). In PS3, the simulation of HOVs traveling through the network resulted in the lowest emissions of CO_2 and NOx when compared to the baseline layout. Specifically, the percentage reduction in CO_2 and NOx emissions for PS3 in comparison to the base layout amounted to 12% and 13%, respectively. Analyzing the results from the TSB simulation, as presented thus far, we can also conclude that PS3 stands out as an energy-efficient alternative that effectively combines the favorable aspects of CAVs and TCMs.

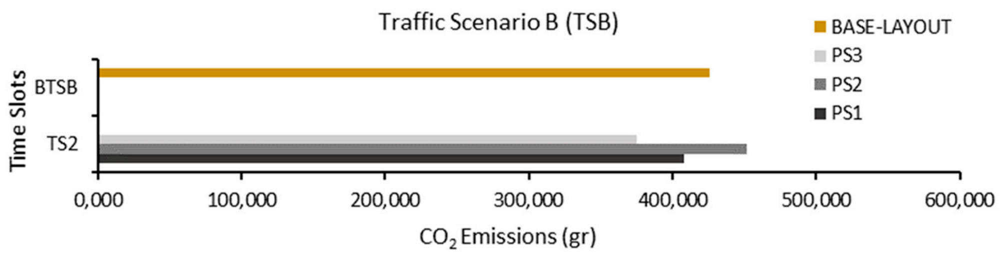

(**a**)

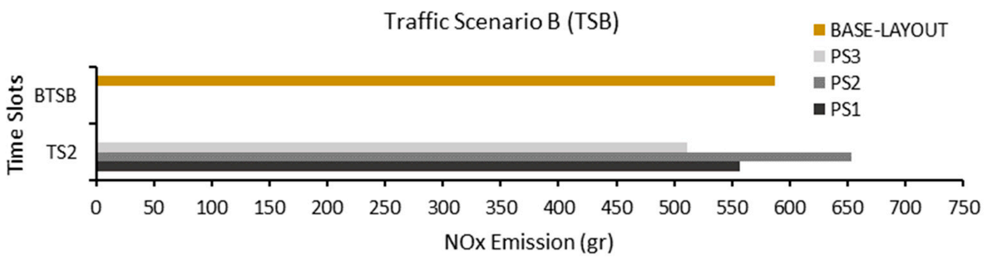

(**b**)

Figure 13. Simulated pollution emissions: (**a**) HOVs' CO_2 pollution values in grams returned by Aimsun in traffic scenario B (TSB); (**b**) HOVs' NOx pollution values in grams returned by Aimsun in traffic scenario B (TSB). Note that PS1, PS2, and PS3 are Project Solutions 1, 2, and 3, respectively; BTSB stands for baseline traffic scenario B; TS2 stands for Time Slot 2.

The safety performances of the three urban road design solutions, which incorporate traffic-calming measures and CDTs, was evaluated using surrogate safety measures. Trajectory files generated by Aimsun Next were processed by the Surrogate Safety Assessment

Model (SSAM) to determine the number of potential conflicts. The results of the safety analysis are presented in Figure 14, which illustrates the total number of potential conflicts that occurred during the simulation of TSA and TSB (see Tables 2 and 3).

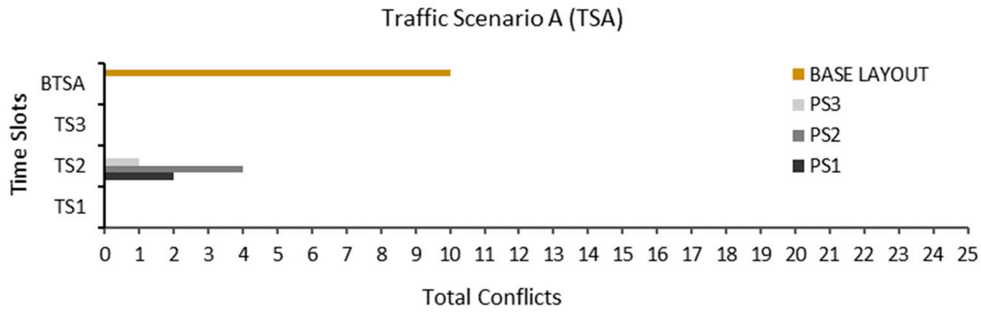

(**a**)

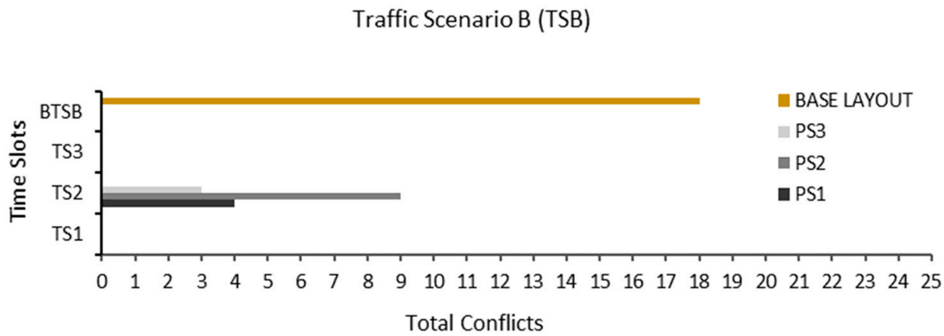

(**b**)

Figure 14. Total potential conflicts occurred in the simulation of traffic scenarios during Time Slot 2 (TS2): (**a**) traffic scenario A (TSA); (**b**) traffic scenario B (TSB). Note that PS1, PS2, and PS3 are Project Solutions 1, 2 and 3, respectively; BTSA and BTSB stand for baseline traffic scenarios A and B, respectively; TS1, TS2, and TS3 stand for Time Slots 1, 2, and 3, respectively.

Specifically, Figure 14a compares the number of conflicts that occurred during TS2 for each project solution with BTSA, as outlined in the organization plan (see Tables 2 and 3). Figure 14a demonstrates that in comparison to the base layout, PS3 had the lowest number of simulated conflicts with a remarkable 90% reduction in total conflicts. Similar results were obtained when simulating TSB with PS3 showing a significantly lower number of conflicts compared to the base layout (see Figure 14b). Finally, the results indicate that all the design solutions incorporating TCMs in combination with CDTs are safer than the current road layout. However, the safety analysis of these design solutions underscores that PS3 is the safest alternative, as it returned the lowest total number of conflicts. Notably, the design of PS3, which includes a dedicated lane for shuttle buses adjacent to the sidewalk, reduces potential conflicts with turning flows entering or exiting the road network.

5. Discussion

The current era of urban development is ushering in new and appealing horizons in the field of urban road planning. This transformation requires designers and decision makers to propose energy-efficient solutions that make urban road spaces eco-sustainable, technologically advanced, healthy, and safe. While traffic-calming measures (TCMs) have been in place for several years, they have gained renewed attention as a successful strategy to address the evolving challenges of energy-efficient and smart cities. Numerous studies have emphasized the potential benefits of TCMs in mitigating the adverse impacts of motorized traffic on urban centers, ultimately enhancing general traffic conditions and the overall well-being of citizens [3,11,57–59].

Indeed, TCMs aim at reclaiming urban road space, reducing traffic noise and emissions, improving air quality, achieving energy savings, and decreasing potential conflicts among road users [13–15]. While these measures offer numerous benefits, they need to incorporate digital technologies to keep pace with the development of smart cities. Cooperative CDTs represent one of the most promising innovations in the automotive field. They are designed to reduce drivers' workloads, optimize traffic flows through digital communications, and minimize environmental emissions [43]. However, the synergistic effects of integrating TCMs with CDTs have not been extensively explored. To address this gap, this study aims to investigate the impacts of TCM-based road solutions featuring CDTs in the transition toward increasingly energy-efficient and smart cities. For this study, a specific area was chosen, and three alternative project solutions that combine TCMs with CDTs were designed and compared to the base layout in a controlled environment (see Figure 6).

To achieve this, Aimsun Next was employed to replicate the driving behavior of CAVs in traffic. Given the absence of high levels of automation and connectivity, the capacity adjustment factors for CAVs on roundabouts, as provided by the Highway Capacity Manual (HCM) [50], were utilized to adjust the capacity curves, which were then used as target values [51].

The results of the model parameter fine-tuning process, as shown in Table 5, demonstrated a strong alignment between the simulated capacity data and the target curves, as depicted in Figure 7. Consequently, a robust microsimulation model of the network under examination was developed. This model featured TCMs, manifested in roundabout installations, and an organized LTZ, with CAVs functioning as a public transport system.

The simulation outputs provided the foundational data for the comparison of each proposed project solution against the base layout in terms of operational, environmental, and safety performances.

The total delay results, obtained by simulating both the TSA and the TSB, consistently demonstrate that PS3 outperformed the other design solutions compared to the base layout, as depicted in Figures 9 and 12. The greater performance of PS3 can be attributed to its specific road platform configuration. In PS3, there are dedicated lanes for each user class admitted to the LTZ, as illustrated in Figure 6c. In contrast, PS1 and PS2 have scenarios where HOVs and shuttle buses share traffic lanes, resulting in increased delays for users. However, simulations returned lower delay values for PS1 compared to PS2, which is primarily because PS1 also incorporates a reserved traffic lane for shuttle buses in the east–west direction, as seen in Figure 6a,b.

Similar patterns emerge when examining pollutant emissions of CO_2 and NOx simulated in Aimsun Next. In both traffic scenarios, TSA and TSB, the emissions produced by HOVs were notably lower in PS3 compared to the other project solutions (see Figures 10 and 13). This outcome can be attributed to the reduced travel delay. With smaller delays, traffic flows move more smoothly on the network, resulting in fewer stop-and-go actions by drivers and a subsequent decrease in vehicular pollutant emissions and, consequently, energy consumption (e.g., [4]).

It is crucial to derive vehicle speed profiles to gain a better understanding of speed variations and their direct implications for the amount of pollutant emissions from motorized traffic. Furthermore, the safety analysis of the three designed solutions, conducted through surrogate safety measures, unequivocally favored PS3.

In PS3, the number of total conflicts observed was notably lower than in the base layout. Despite both PS3 and the base layout sharing a similar road platform configuration, this difference in potential conflicts can be attributed to the presence of two roundabouts in PS3 compared to just one roundabout in the base layout along with the simulated delays. Roundabout intersections have been shown to enhance road safety by reducing the number of conflicts and their severity compared to unsignalized intersections [4]. However, the high delay values experienced while traveling through the network could lead to more assertive driving behavior, subsequently increasing the risk of collisions with other users.

It would be valuable to explore the speed trends at various points in the network to establish a comprehensive understanding of the relationship between emissions, speed variations, and the number of potential conflicts. Future research developments in our study may also involve an analysis of the speed profiles exhibited by vehicles alongside connected and autonomous vehicles in the road network where traffic-calming measures are implemented.

Two synthesis graphs are provided below to evaluate the overall operational, environmental, and safety performances of the three design solutions compared to the basic layout. Figure 15a,b depict the performance trends of the three design solutions simulated under TSA and TSB conditions. In both traffic scenarios, PS3 stands out as the only one among the three design alternatives to achieve a reduction in delay. Additionally, regarding emissions, Figure 15 makes it evident that compared to the other alternatives, PS3 is the most eco-friendly solution. Moreover, Figure 15 highlights that each design solution results in a decrease in total conflicts compared to the base solution. In conclusion, based on the overall results presented in Figure 15a,b, it is evident that PS3 represents an appropriate urban design solution well-suited to combine the positive effects of TCMs with CDTs from an energy efficiency perspective. Based on the results discussed above, TCMs featuring CDTs could be promising solutions toward new environmental sustainability goals in urban centers and tourist-oriented cities. These solutions focus on providing safe, operationally functional, and appealing shared road spaces. In this era of cities in transition, this combination offers an opportunity for urban renewal, where urban street redesign, traffic flow management, and the reclamation of road space are designed on a human scale.

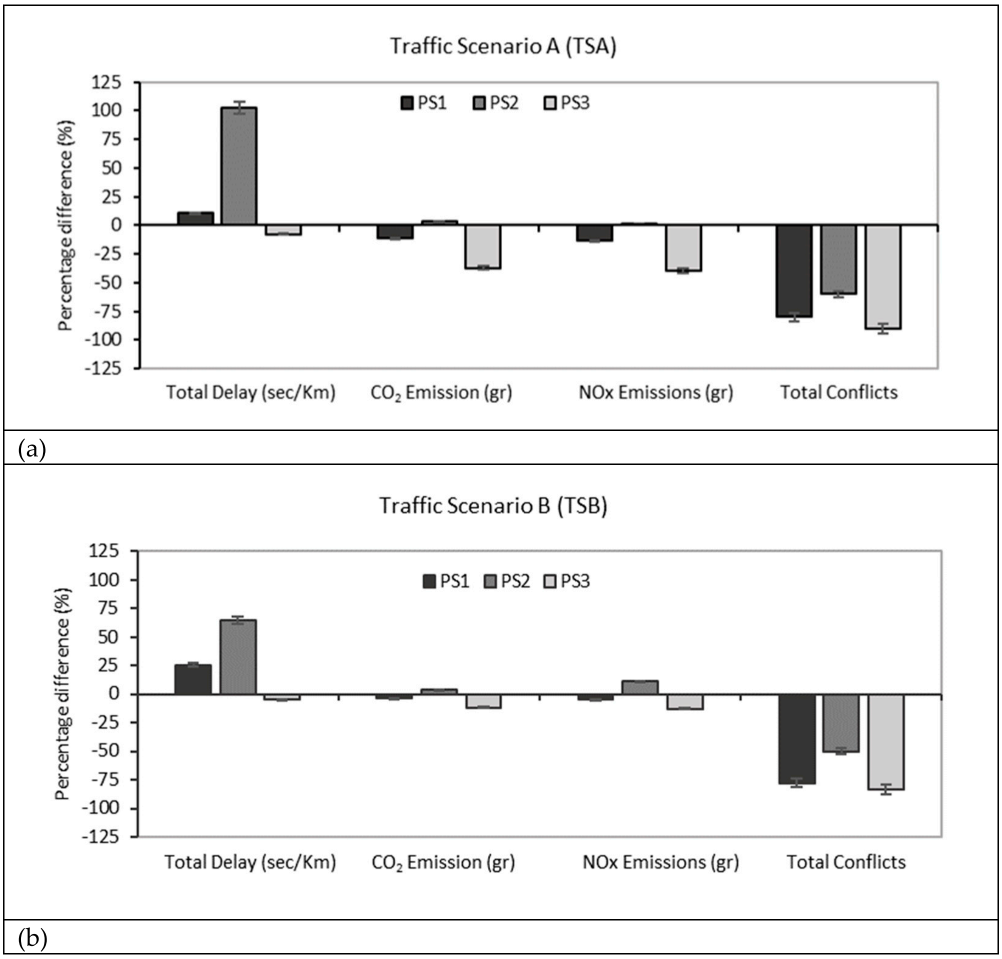

Figure 15. The overall operational, environmental and safety performances of the three design solutions compared to the basic layout: (**a**) traffic scenario A (TSA); (**b**) traffic scenario B (TSB). Note that PS1, PS2, PS3 are Project Solutions 1, 2 and 3, respectively.

6. Conclusions

Traffic-calming strategies have a central goal of reducing vehicle speeds and enhancing traffic safety, thereby contributing to the creation of more pedestrian-friendly and livable urban spaces [11–13]. When these measures are seamlessly integrated into urban road design, cities can foster safer streets that discourage reckless driving while promoting a more considerate and energy-efficient approach to road use. Furthermore, cooperative driving technologies complement traffic-calming endeavors by making use of vehicle-to-vehicle (V2V) and vehicle-to-infrastructure (V2I) communication [43,60]. These technologies empower vehicles to share real-time information, including data on traffic conditions, potential hazards, and optimal routes. This sharing enables vehicles to synchronize their movements, resulting in smoother traffic flow, reduced congestion, and enhanced overall efficiency. Additionally, smart city infrastructures can be equipped with an array of sensors and cameras to continuously gather real-time traffic data, which can then be processed by machine learning algorithms. These algorithms are designed to identify traffic patterns, evaluate performance, and provide data-driven recommendations for improvements.

In the context of smart city and energy efficiency transitions, the evaluation of such integrated solutions is crucial to ensure their effectiveness and alignment with city objectives. This research is focused on evaluating traffic-calming-based urban road design solutions that incorporate cooperative driving technologies from both safety and efficiency perspectives.

The micro-simulation approach employed in this case study facilitated the early assessment and comparison of the operational and safety performances of three environmentally friendly design solutions involving traffic-calming measures (TCMs) and cooperative driving technologies (CDTs). In the tourist-oriented coastal area chosen as the case study, three distinct project solutions were developed, incorporating LTZs and roundabout installations as TCMs. Cooperative driving systems, with a fully electric power supply, were utilized to provide public transport services in the seaside area.

Within the simulation environment, calibration of the model parameters for CAVs was necessary to accurately replicate their real-world driving behavior. The results of micro-simulation allowed for a comparison of the three designed solutions with the current conditions. The operational and environmental performance of these various design solutions, assessed in a controlled environment, laid the groundwork for comparing each design alternative with the existing conditions. Among the three design solutions, PS3 emerged as the most promising in terms of both operational efficiency and environmental impact. It reduced delays and generated the least amount of polluting emissions compared to the current situation. It is worth noting that the driving behavior of road users, influenced by both internal and external factors affecting traffic flows, significantly impacts vehicle emissions even within a simulation environment [61,62]. Pollutant emissions tend to increase with higher average vehicle speeds and during sudden acceleration or deceleration maneuvers [63]. Future research should delve into vehicle speed profiles to gain a deeper understanding of how traffic-calming devices affect speed variations and their implications for pollutant emissions, fuel consumption, and energy use.

Despite the fact that the traffic-calming measures in this case study did not necessitate abrupt acceleration or deceleration maneuvers, investigating the environmental effects of speed variations at roundabouts where the right of way is negotiated at entries would be interesting. From a road safety perspective, the installation of roundabouts as TCMs resulted in a reduction in potential conflicts for all three simulated project solutions compared to the base layout. Furthermore, since the three design solutions featured varying road platform layouts, an exploration was conducted to determine which of them was the safest and most eco-friendly. The safety analysis, conducted through surrogate measures, enabled the evaluation of the safest alternative. PS3 was identified as the safest design solution due to its dedicated lane for shuttle buses positioned alongside the sidewalk, reducing potential conflicts with turning traffic entering or exiting the road network.

City planners and policymakers, when proposing novel and innovative design solutions in alignment with the goals of transitioning to energy-efficient and smart cities, have to conduct comprehensive assessments. These assessments should encompass various factors, including their impact on traffic flow, potential reductions in traffic crashes, changes in air quality, and public acceptance. Moreover, they should take into account the feasibility of implementation, associated costs, and any challenges that may arise. In the near future, a cost–benefit analysis should be conducted to evaluate the overall costs over the life cycle of each design proposal, providing valuable insights for decision makers [64,65]. In this regard, the costs of these interventions could potentially be offset by revenue generated from ticket sales for parking and the use of public transportation services by road users. Additional income streams could be established by introducing services such as bike sharing, which aligns well with the principles of the LTZ.

Furthermore, these planned measures can enhance the overall appeal of the bathing area, benefitting both tourists and residents. This improved quality of life extends beyond economic gains. Offering road users safe, healthy, well-designed, and visually appealing road spaces that seamlessly integrate with the surrounding environment can incentivize the use of public shared transportation over private vehicles [17].

Public engagement and community involvement play a crucial role in the success of these initiatives. Citizen feedback provides valuable insights into the practicality and acceptance of these solutions. Additionally, cities must address ethical considerations related to technologies, including data privacy and cybersecurity concerns.

In conclusion, the integration of traffic-calming-based urban road design solutions with cooperative driving technologies holds significant potential for advancing energy-efficient and smart city transitions. While a cost analysis is necessary for the near future to assess the life-cycle costs of each design proposal and support decision making, this research can contribute to the enhancement of urban mobility strategies. The combination of connected and autonomous vehicles with traffic-calming measures can effectively reduce fuel consumption, emissions, and energy waste, leading to a more environmentally friendly transportation system. By creating safer, more efficient, and sustainable mobility solutions, these integrated approaches contribute to the development of cities that are not only livable and eco-friendly but also technologically advanced. However, the successful implementation of these solutions requires a thorough evaluation, data analysis, public participation, and collaboration among government entities, industry stakeholders, and the community at large.

Author Contributions: Conceptualization, M.L.T., E.M., A.G. and T.G.; methodology, M.L.T., E.M., A.G. and T.G.; software, M.L.T., E.M., A.G. and T.G.; validation, M.L.T., E.M., A.G. and T.G.; formal analysis, M.L.T., E.M., A.G. and T.G.; investigation, M.L.T., E.M., A.G. and T.G.; resources, M.L.T., E.M., A.G. and T.G.; data curation, M.L.T., E.M., A.G. and T.G.; writing—original draft preparation, M.L.T., E.M., A.G. and T.G.; writing—review and editing, M.L.T., E.M., A.G. and T.G.; visualization, M.L.T., E.M., A.G. and T.G.; supervision, E.M., A.G. and T.G.; project administration, M.L.T., E.M., A.G. and T.G.; funding acquisition, M.L.T., E.M., A.G. and T.G. All authors have read and agreed to the published version of the manuscript.

Funding: This research received no external funding.

Data Availability Statement: Data are available after kind request to the corresponding author.

Acknowledgments: Sustainable Mobility Center (Centro Nazionale per la Mobilità Sostenibile—CNMS) under Grant CN00000023 CUP B73C22000760001.

Conflicts of Interest: The authors declare no conflict of interest.

References

1. Ambros, J.; Tomešová, L.; Jurewicz, C.; Valentová, V. A review of the best practice in traffic calming evaluation. *Accid. Anal. Prev.* **2023**, *189*, 107073. [CrossRef] [PubMed]
2. Paszkowski, J.; Herrmann, M.; Richter, M.; Szarata, A. Modelling the Effects of Traffic-Calming Introduction to Volume–Delay Functions and Traffic Assignment. *Energies* **2021**, *14*, 3726. [CrossRef]
3. Gonzalo-Orden, H.; Rojo, M.; Pérez-Acebo, H.; Linares, A. Traffic calming measures and their effect on the variation of speed. *Transp. Res. Procedia* **2016**, *18*, 349–356. [CrossRef]

4. National Academies of Sciences, Engineering, and Medicine. *Roundabouts: An Informational Guide*, 2nd ed.; The National Academies Press: Washington, DC, USA, 2010.
5. Seuwou, P.; Banissi, E.; Ubakanma, G. The Future of Mobility with Connected and Autonomous Vehicles in Smart Cities. In *Digital Twin Technologies and Smart Cities. Internet of Things*; Farsi, M., Daneshkhah, A., Hosseinian-Far, A., Jahankhani, H., Eds.; Springer: Cham, Switzerland, 2020; Volume 1, pp. 37–52. [CrossRef]
6. Tumminello, M.L.; Macioszek, E.; Granà, A.; Giuffrè, T. A Methodological Framework to Assess Road Infrastructure Safety and Performance Efficiency in the Transition toward Cooperative Driving. *Sustainability* **2023**, *15*, 9345. [CrossRef]
7. Rana, M.M.; Hossain, K. Connected and Autonomous Vehicles and Infrastructures: A Literature Review. *Int. J. Pavement Res. Technol.* **2023**, *16*, 264–284. [CrossRef]
8. Anagnostopoulos, A.; Kehagia, F. CAVs and roundabouts: Research on traffic impacts and design elements. *Transp. Res. Procedia* **2020**, *49*, 83–94. [CrossRef]
9. Aimsun Next. *Version 20 Dynamic Simulator User Manual*; TSS-Transport Simulation Systems: Barcelona, Spain, 2020.
10. Gettman, D.; Pu, L.; Sayed, T.; Shelby, S.G. *Surrogate Safety Assessment Model and Validation: Final Report*; Georgetown Pike (US) Report FHWA HRT 08–051; Federal Highway Administration: Washington, DC, USA, 2008.
11. Chng, S.; Chang, C.; Mosquera, K.; Leong, W.Y. Living in a Silver Zone: Residents' perceptions of area-wide traffic calming measures in Singapore. *Transp. Res. Interdiscip. Perspect.* **2022**, *16*, 100710. [CrossRef]
12. Cantisani, G.; Corazza, M.V.; Di Mascio, P.; Moretti, L. Eight Traffic Calming "Easy Pieces" to Shape the Everyday Pedestrian Realm. *Sustainability* **2023**, *15*, 7880. [CrossRef]
13. Damsere-Derry, J.; Lumor, R.; Bawa, S.; Tikoli, D. Effects of traffic Calming measures on mobility, road safety and pavement conditions on Abuakwa-Bibiani highway. *Front. Sustain. Cities* **2020**, *2*, 26. [CrossRef]
14. Juhász, M.; Koren, C. Getting an insight into the effects of traffic calming measures on road safety. *Transp. Res. Procedia* **2016**, *14*, 3811–3820. [CrossRef]
15. Juhász Bunn, F.; Collier, T.; Frost, C.; Ker, K.; Roberts, I.; Wentz, R. Traffic calming for the prevention of road traffic injuries: Systematic review and meta-analysis. *Inj. Prev.* **2003**, *9*, 200–204. [CrossRef] [PubMed]
16. Giuffre', O.; Grana', A.; Giuffre', T.; Marino, R. Emission factors related to vehicle modal activity. *Int. J. Sustain. Dev. Plan.* **2011**, *6*, 447–458. [CrossRef]
17. Balant, M.; Lep, M. Comprehensive Traffic Calming as a Key Element of Sustainable Urban Mobility Plans—Impacts of a Neighbourhood Redesign in Ljutomer. *Sustainability* **2020**, *12*, 8143. [CrossRef]
18. Chaves, C.; Vasconcelos, A.L.; Bastos Silva, A.; Almeida, R. Microsimulation–based evaluation of a 30 km/h zone. In *Road and Rail Infrastructure, V.*; Lakusic, S., Ed.; Tiskara Zelina: Zadar, Croatia, 2018; pp. 1341–1347.
19. Elvik, R. Area-wide urban traffic calming schemes: A meta-analysis of safety effects. *Accid. Anal. Prev.* **2001**, *33*, 327–336. [CrossRef] [PubMed]
20. Jateikienė, L.; Andriejauskas, T.; Lingytė, I.; Jasiūnienė, V. Impact assessment of speed calming measures on road safety. *Transp. Res. Procedia* **2016**, *14*, 4228–4236. [CrossRef]
21. Lee, G.; Joo, S.; Oh, C.; Choi, K. An evaluation framework for traffic calming measures in residential areas. *Transp. Res. Part D Transp. Environ.* **2013**, *25*, 68–76. [CrossRef]
22. Ariën, C.; Jongen, E.M.; Brijs, K.; Brijs, T.; Daniels, S.; Wets, G. A simulator study on the impact of traffic calming measures in urban areas on driving behavior and workload. *Accid. Anal. Prev.* **2013**, *61*, 43–53. [CrossRef] [PubMed]
23. Distefano, N.; Leonardi, S. Evaluation of the benefits of traffic calming on vehicle speed reduction. *Civ. Eng. Archit.* **2019**, *7*, 200–214. [CrossRef]
24. Aydin, M.M.; Gunay, B.; Akgol, K. Performance Comparison of Various Chicane Types: A Driving Simulator Study. *Int. J. Civ. Eng.* **2019**, *17*, 1753–1765. [CrossRef]
25. Abdulmawjoud, A.A.; Jamel, M.G.; Al-Taei, A.A. Traffic flow parameters development modelling at traffic calming measures located on arterial roads. *Ain Shams Eng. J.* **2021**, *12*, 437–444. [CrossRef]
26. Akbari, A.; Haghighi, F. Traffic calming measures: An evaluation of four low-cost TCMs' effect on driving speed and lateral distance. *IATSS Res.* **2020**, *44*, 67–74. [CrossRef]
27. Vaitkus, A.; Čygas, D.; Jasiūnienė, V.; Jateikienė, L.; Andriejauskas, T.; Skrodenis, D.; Ratkevičiūtė, K. Traffic calming measures: An evaluation of the effect on driving speed. *Promet-Traffic Transp.* **2017**, *29*, 275–285. [CrossRef]
28. Pérez-Acebo, H.; Ziółkowski, R.; Linares-Unamunzaga, A.; Gonzalo-Orden, H. A series of vertical deflections, a promising traffic calming measure: Analysis and recommendations for spacing. *Appl. Sci.* **2020**, *10*, 3368. [CrossRef]
29. Pazzini, M.; Lantieri, C.; Vignali, V.; Dondi, G.; Giovannini, A.; Mora, A. Road users' behaviour in the "30 km/h zones". The case study of Bologna. *Transp. Res. Procedia* **2023**, *69*, 504–511. [CrossRef]
30. Distefano, N.; Leonardi, S. Evaluation of the effectiveness of traffic calming measures by SPEIR methodology: Framework and case studies. *Sustainability* **2022**, *14*, 7325. [CrossRef]
31. García, A.; Torres, A.J.; Romero, M.A.; Moreno, A.T. Traffic microsimulation study to evaluate the effect of type and spacing of traffic calming devices on capacity. *Procedia-Soc. Behav. Sci.* **2011**, *16*, 270–281. [CrossRef]
32. Shirmohammadi, H.; Mardani, E.; Emdadian Ghane, M.; Hasheminezhad, A. Simulating the Effects of Type and Spacing of Traffic Calming Measures on Urban Road Capacity. *Int. J. Transp. Eng.* **2018**, *6*, 65–83.

33. Ghafghazi, G.; Hatzopoulou, M. Simulating the air quality impacts of traffic calming schemes in a dense urban neighborhood. *Transp. Res. Part D Transp. Environ.* **2015**, *35*, 11–22. [CrossRef]
34. Pérez-Sansalvador, J.C.; Lakouari, N.; Garcia-Diaz, J.; Hernández, S.E.P. The Effect of Speed Humps on Instantaneous Traffic Emissions. *Appl. Sci.* **2020**, *10*, 1592. [CrossRef]
35. Januševičius, T.; Grubliauskas, R. The effect of speed bumps and humps on the concentrations of CO, NO and NO_2 in ambient air. Air Quality. *Atmos. Health* **2019**, *12*, 635–642. [CrossRef]
36. Ghafghazi, G.; Hatzopoulou, M. Simulating the environmental effects of isolated and area-wide traffic calming schemes using traffic simulation and microscopic emission modeling. *Transportation* **2014**, *41*, 633–649. [CrossRef]
37. Ahac, S.; Ahac, M.; Domitrović, J.; Dragčević, V. Modeling the influence of roundabout deflection on its efficiency as a noise abatement measure. *Sustainability* **2021**, *13*, 5407. [CrossRef]
38. Džambas, T.; Dragčević, V.; Lakušić, J. Impact of vertical traffic calming devices on environmental noise. *Građevinar* **2020**, *12*, 1131–1143.
39. El-Bardisy, N.; Elshater, A.; Afifi, S.; Alfiky, A. Predicting traffic sound levels in Cairo before, during, and after the COVID-19 lockdown using Predictor-LimA software. *Ain Shams Eng. J.* **2023**, *14*, 102088. [CrossRef]
40. Ariën, C.; Brijs, K.; Brijs, T.; Ceulemans, W.; Vanroelen, G.; Jongen, E.M.M.; Daniels, S.; Wets, G. Does the effect of traffic calming measures endure over time? A simulator study on the influence of gates. *Transp. Res. Part F Traffic Psychol. Behav.* **2014**, *22*, 63–75. [CrossRef]
41. Mauro, R. *Calculation of Roundabouts. Capacity, Waiting Phenomena and Reliability*; Springer: Berlin/Heidelberg, Germany, 2010.
42. Rahman, M.M.; Thill, J.C. Impacts of Connected and Autonomous Vehicles on Urban Transportation and Environment: A Comprehensive Review. *Sustain. Cities Soc.* **2023**, *96*, 104649. [CrossRef]
43. Brost, M.; Deniz, Ö.; Österle, I.; Ulrich, C.; Senzeybek, M.; Hahn, R.; Schmid, S. Energy Consumption of Connected and Automated Vehicles. In *Electric, Hybrid, and Fuel Cell Vehicles, Encyclopedia of Sustainability Science and Technology*, 2nd ed.; Elgowainy, A., Ed.; Springer: New York, NY, USA, 2021; pp. 216–224.
44. Karbasi, A.; O'Hern, S. Investigating the impact of connected and automated vehicles on signalized and unsignalized intersections safety in mixed traffic. *Future Transp.* **2022**, *2*, 24–40. [CrossRef]
45. Elawady, A.; Abuzwidah, M.; Zeiada, W. The Benefits of Using Connected Vehicles System on Traffic Delay and Safety at Urban Signalized Intersections. In Proceedings of the 2022 Advances in Science and Engineering Technology International Conferences (ASET), Dubai, United Arab Emirates, 21–24 February 2022; pp. 1–6. [CrossRef]
46. Mavromatis, I.; Tassi, A.; Piechocki, R.J.; Sooriyabandara, M. On Urban Traffic Flow Benefits of Connected and Automated Vehicles. In Proceedings of the 2020 IEEE 91st Vehicular Technology Conference (VTC2020-Spring), Antwerp, Belgium, 25–28 May 2020; pp. 1–7. [CrossRef]
47. Ye, L.; Yamamoto, T. Evaluating the impact of connected and autonomous vehicles on traffic safety. *Phys. A Stat. Mech. Its Appl.* **2019**, *526*, 121009. [CrossRef]
48. Chehri, A.; Mouftah, H.T. Autonomous vehicles in the sustainable cities, the beginning of a green adventure. *Sustain. Cities Soc.* **2019**, *51*, 101751. [CrossRef]
49. Italian Minister of Infrastructure and Transport. *Functional and Geometric Standards for Road Intersections*; Italian Minister of Infrastructure and Transport: Rome, Italy, 2006.
50. National Academies of Sciences, Engineering, and Medicine. *Highway Capacity Manual 7th Edition: A Guide for Multimodal Mobility Analysis*; The National Academies Press: Washington, DC, USA, 2022.
51. Barceló, J. *Fundamentals of Traffic Simulation*; Springer: London, UK, 2010.
52. Gipps, P.G. A Behavioural Car-Following Model for Computer Simulation. *Transp. Res. Part B* **1981**, *15*, 105–111. [CrossRef]
53. Abedian, S.; Mirsanjari, M.M.; Salmanmahiny, A. Investigating the effect of suburban buses on traffic flow and carbon monoxide emission by Aimsun simulation software. *J. Indian Soc. Remote Sens.* **2021**, *49*, 1319–1330. [CrossRef]
54. Giuffrè, O.; Granà, A.; Tumminello, M.L.; Giuffrè, T.; Trubia, S.; Sferlazza, A.; Rencelj, M. Evaluation of roundabout safety performance through surrogate safety measures from microsimulation. *J. Adv. Transp.* **2018**, *2018*, 4915970. [CrossRef]
55. Saleem, T.; Persaud, B.; Shalaby, A.; Ariza, A. Can Microsimulation Be Used to Estimate Intersection Safety?: Case Studies Using VISSIM and Paramics. *Transp. Res. Rec. J. Transp. Res. Board* **2014**, *2432*, 142–148. [CrossRef]
56. Oikonomou, M.G.; Ziakopoulos, A.; Chaudhry, A.; Thomas, P.; Yannis, G. From conflicts to crashes: Simulating macroscopic connected and automated driving vehicle safety. *Accid. Anal. Prev.* **2023**, *187*, 107087. [CrossRef] [PubMed]
57. Wang, J.; Ying, J.; Jiang, S. An Adaptive Traffic-Calming Measure and Effectiveness Evaluation in a Large Urban Complex of Shanghai, China. *Sustainability* **2022**, *14*, 13023. [CrossRef]
58. Pérez-Acebo, H.; Ziolkowski, R.; Gonzalo-Orden, H. Evaluation of the Radar Speed Cameras and Panels Indicating the Vehicles' Speed as Traffic Calming Measures (TCM) in Short Length Urban Areas Located along Rural Roads. *Energies* **2021**, *14*, 8146. [CrossRef]
59. Solowczuk, A. Effect of Traffic Calming in a Downtown District of Szczecin, Poland. *Energies* **2021**, *14*, 5838. [CrossRef]
60. Dong, C.; Wang, H.; Li, Y.; Liu, Y.; Chen, Q. Economic comparison between vehicle to vehicle (V2V) and vehicle to infrastructure (V2I) at freeway on ramps based on microscopic simulations. *IET Intell. Transp. Syst.* **2019**, *13*, 1726–1735.
61. Shahariar, G.H.; Sajjad, M.; Suara, K.A.; Jahirul, M.I.; Chu-Van, T.; Ristovski, Z.; Bodisco, T.A. On-road CO2 and NOx emissions of a diesel vehicle in urban traffic. *Transp. Res. Part D Transp. Environ.* **2022**, *107*, 103326. [CrossRef]
62. Mądziel, M. Vehicle Emission Models and Traffic Simulators: A Review. *Energies* **2023**, *16*, 3941. [CrossRef]

63. Belkacem, I.; Helali, A.; Khardi, S.; Slimi, K. Investigations on vehicle non-exhaust particle emissions: Real-time measurements. *Int. J. Environ. Sci. Technol.* **2022**, *19*, 11749–11762. [CrossRef]
64. Jazcilevich, A.; Mares Vázquez, J.M.; Ramírez, P.L.; Pérez, I.R. Economic-environmental analysis of traffic-calming devices. *Transp. Res. Part D Transp. Environ.* **2015**, *36*, 86–95. [CrossRef]
65. Alogdianakis, F.; Dimitriou, L. In-Depth Appraisal of Bus Transport Services for Sustainability Performance: A Cost–Benefit Analysis Approach. *Transp. Res. Rec.* **2023**. [CrossRef]